A STUDY OF END-BLOCKS FOR POST-TENSIONED BEAMS

by 632

TAHER F. GINWALA

B. E. (Civil), Poona University, India, 1969

A MASTER'S REPORT

submitted in partial fulfillment of the

requirements for the degree

MASTER OF SCIENCE

Department of Civil Engineering

KANSAS STATE UNIVERSITY
Manhattan, Kansas

1970

Approved by:

Vernon H. Rousenaugh
Major Professor

TABLE OF CONTENTS

LIST OF FIGURES

LIST OF TABLES

SYNOPSIS

The stress distribution in end-blocks of post-tensioned prestressed concrete beams has become important due to extensive use of prestressed concrete beams. An attempt has been made to present the research work of some predominant authorities on this topic in this writing.

The following three approaches have been identified in this report: 1) the two-dimensional analysis by Y. Guyon, 2) the two-dimensional analysis by Sundra Raja Iyengar, and 3) the physical analog method by R. J. Lenschow and M. A. Sozen.

Finally, comparison of these methods has been made by solving numerical examples. The methods are also compared with photoelastic investigation by S. P. Christodoulides.

INTRODUCTION

The development of the technique of prestressed concrete in modern construction is becoming more and more important due to its multifold advantages, such as 1) high durability due to the use of high strength concrete, and the absence of cracking, 2) long span beams, with economical cross section, which greatly help when bridges are located over soils unsuited for foundation support by eliminating the need for intermediate piers, 3) quickness in erection and reduction of falsework. With the increase in transport facilities and lifting devices capable of handling them, prestressed beams and slabs are used extensively in the modern world.

In very long prestressed beams and slabs, heavy prestressing forces are transferred at the ends. Hence investigation of the stresses at the ends of beams becomes very important. This problem is of general character and is not confined solely to prestressed beams, but with these it attains considerable importance owing to the magnitude of the forces involved.

Lack of complete knowledge of this problem does not prevent our designing such beams and slabs but this uncertainty results in increased cost as we apply higher factors of safety in our designs. To find an exact solution, and then to provide the exact amount of reinforcement, becomes too laborious and will not be of practical use. Hence the better solution is to use some approximation which will be quicker to solve and will lead to a change in the result on the safe side by an acceptable percentage. This has been attempted by Y. Guyon, G. Magnel, Lenschow and Sozen and other authors. Each one has used his own approach to satisfactorily approximate exact solutions.

The writer of this report has made an attempt to present and compare the approaches of Y. Guyon, R. J. Lenschow and M. A. Sozen, and exact two-dimensional analysis by K. T. Sundra Raja Iyengar. The data are collected from current literature on the subject.

APPROACH OF Y. GUYON[1]

The end-block is the portion of the beam surrounding the anchorage. Within this portion, whose length is approximately equal to the depth of the beam, linear distribution of stress is first attained.

The principle of St. Venant and its experimental verification from photoelasticity indicates that the concentrated load applied on the surface of the beam becomes linearly distributed beyond a certain distance from the end, approximately equal to the depth of the beam.

The assumption made by Guyon is that the external forces, other than the prestress force are negligible, that is to say the beam support is not too close to its end.

The stresses at the surface are concentrated and discontinuous while stresses at the end of the end-blocks are distributed and continuous. This can be done only by giving rise to transverse stresses and shear stresses along the longitudinal plane, which causes tension in certain parts of the block. If the strength of the concrete in tension is not sufficient to take this tension then it becomes necessary to provide reinforcement parallel to the bearing face.

Figure 1 shows the forces on the faces AB and CD of end-block ABCD, under which forces the block is in equilibrium. Block ABCD may be visualized as a deep beam with a linearly distributed load on CD, and supported by P_1 and P_2 as reactions on AB.

Consider any horizontal plane EF. In order to keep BEFC in equilibrium there must exist a normal stress (transverse stress) f_y, and a tangential or

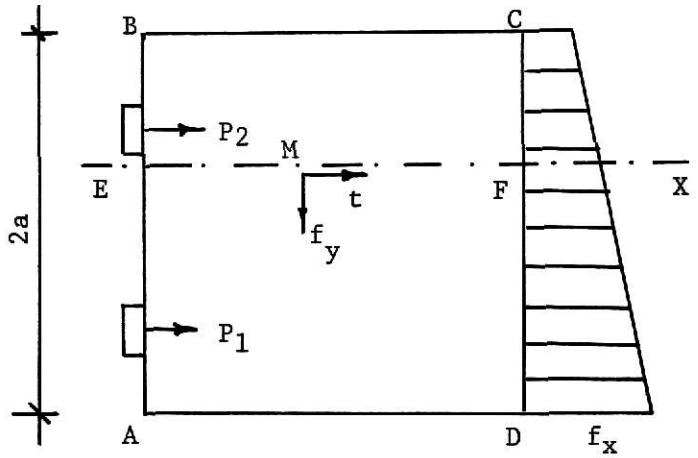

Figure 1. Normal loading of end-block.

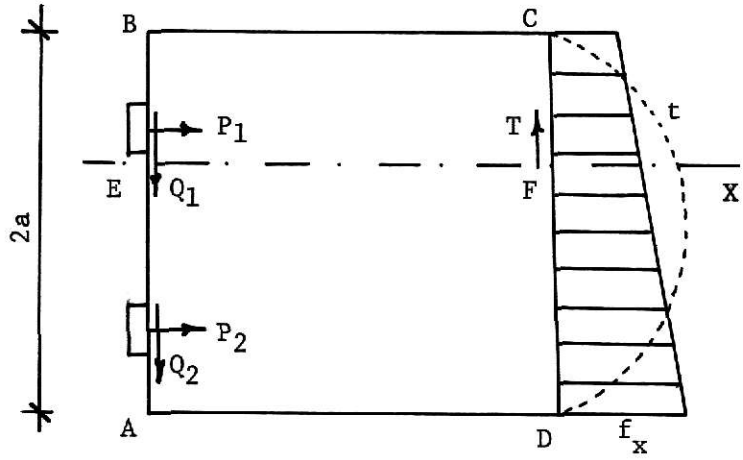

Figure 2. Inclined loading of end-block.

shear stress t on the plane EF.

Consider Fig. 1 with forces normal to AB. The equilibrium will be maintained under the following conditions: 1) The resultant of stresses f_y must be zero. That means the existence along EF of a zone of tension and a zone of compression; 2) The sum of the moment of the stress f_y about a point in EF must equal the sum of the moments of the forces acting on EB and FC,

i. e., in the case of Fig. 1, must equal the difference between the moment of P_2 and the moment of the forces acting on FC; 3) The resultant of the stress t must equal the resultant of horizontal forces applied to BEFC; i. e., in our case the difference between P_2 and the force acting on FC.

If the force on AB is oblique then in addition to normal components P_1, P_2, there exist tangential components Q_1, Q_2, as shown in Fig. 2.

The above mentioned are the conditions which f_y and t must satisfy. Unfortunately, these conditions are not sufficient for the determination of the stress distribution. It is not possible to apply our usual beam theory (a plane section remains plane) to such a short beam. Figures 3 and 4 show general shapes of distribution of stresses f_y and t. The position of zero transverse stress and maximum transverse stress depends on the distribution of load.

To simplify the analysis it is assumed that the load is uniformly distributed along the width of the beam. This reduces the problem from three-dimensional to two-dimensional, and the stress distribution becomes independent of the position of the point considered in the breadth of the beam. Guyon restricts himself to the analysis of the few most unfavorable planes which may be identified in advance by the rules given below.

Case of Single Axial Force

Consider a block of height 2a and unit breadth. As shown in Fig. 5, the single force P is acting over the height 2a' and is symmetrical about the axis of the beam. The end-block is carrying a uniformly distributed load f_x on CD and is supported by the central support P.

The force is considered to pass from AB to CD along isostatic lines as shown in Fig. 5. These isostatic lines have to be normal to AB and CD if f_y

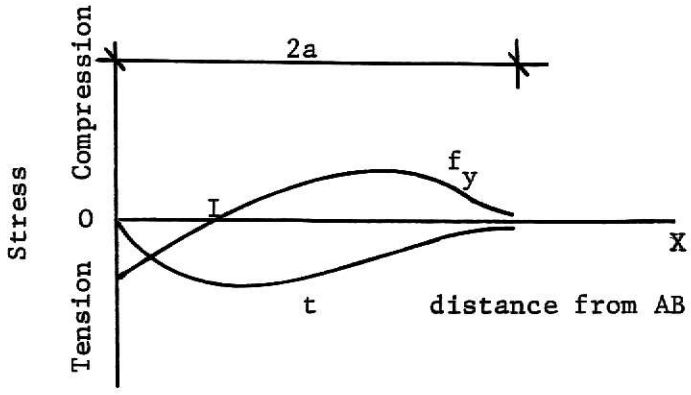

Figure 3. General shape of variation of f_y along load axis.

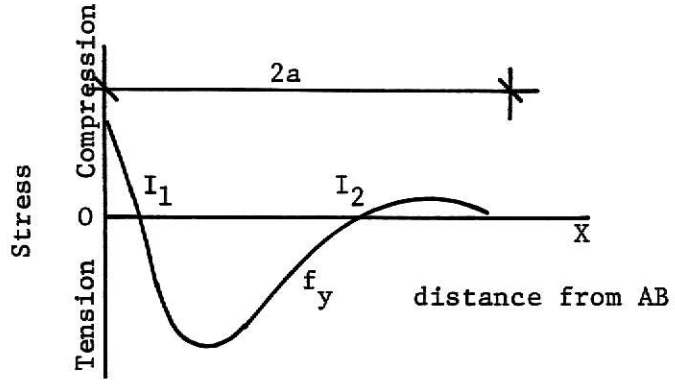

Figure 4. General shape of variation of f_y along other than the load axis.

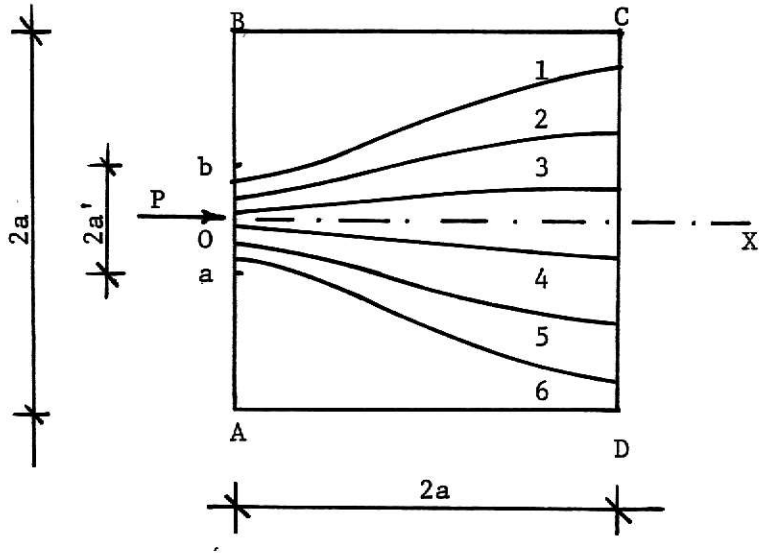

Figure 5. Isostatics of end-block.

is assumed to be zero at these two faces. Between planes AB and CD they adopt an "S" shape. If we divide ab and CD into "n" equal parts, then each isostatic is supposed to carry a force of P/n from the center of one division in ab to the center of one division of CD. These isostatics are curved fibers which will not carry compression without exerting a transverse force normal to the fibers caused by their curvature; this force acts inwards or outwards according to the direction of convexity of the curve. f_y is maximum on the axis as f_y goes on increasing from BC and CD to OX. On OX, t becomes zero due to symmetry. Therefore, on the axis OX the only stress is f_y normal to the axis; its value varies from AB to CD at which point it becomes zero or negligible.

An idea of the variation of f_y along OX may be gained by replacing isostatics on each side of OX by an "average" isostatic carrying $\frac{P}{2}$ to the center of the upper or lower half of CD (Fig. 6).

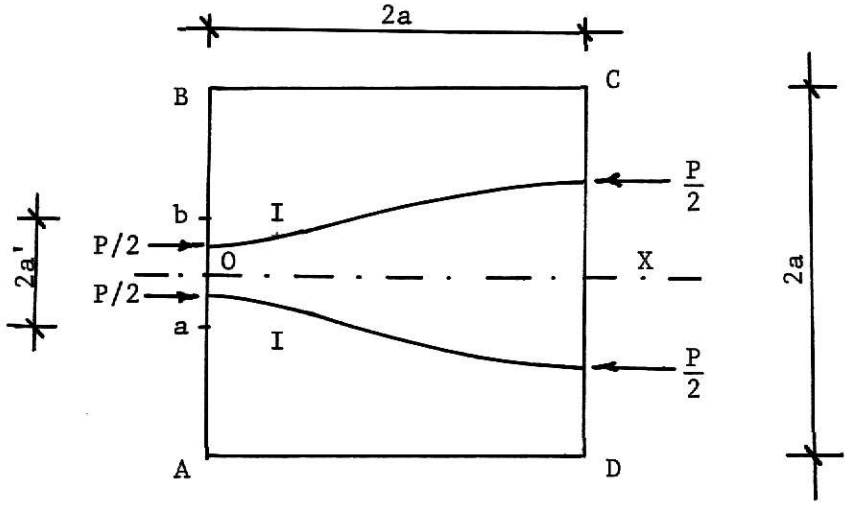

Figure 6. Mean isostatics of end-block.

R is the radius of curvature at any point M. The transverse force per unit length of OX is $\frac{P}{2R}$. There is a point on the curve called I at this

point, R is infinite and hence f_y is zero. From ab to I the R is negative and hence f_y is compressive while between I and CD f_y is tensile. Figures 3 and 4 show the general form of the stress diagram. The area of compression zone and tension zone in the diagram give the resultant compressive and resultant tensile stresses and are equal. They form a couple whose moment should be equal to the moment of the couple formed by P/2 acting on AB, and P/2 acting on CD, i. e., $\frac{P}{2} \times \frac{a-a'}{2}$.

As mentioned above, the value and position of f_y depends on the distribution of force. Figure 7a shows maximum f_y and its position from the face for different ratios of $\frac{a'}{a}$. Thus if the force is concentrated the stress f_y is purely tensile. This contradicts the earlier statement that the positive area under the curve is equal to the negative area. However, the force being ideally concentrated, the compressive stress f_y is of infinite magnitude

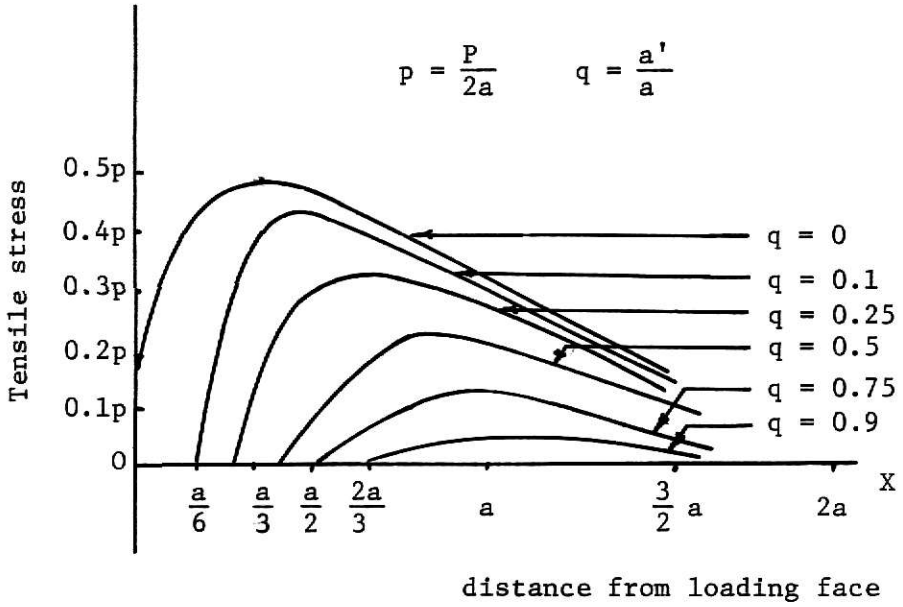

Figure 7a. Distribution of transverse tensile stress along load axis.

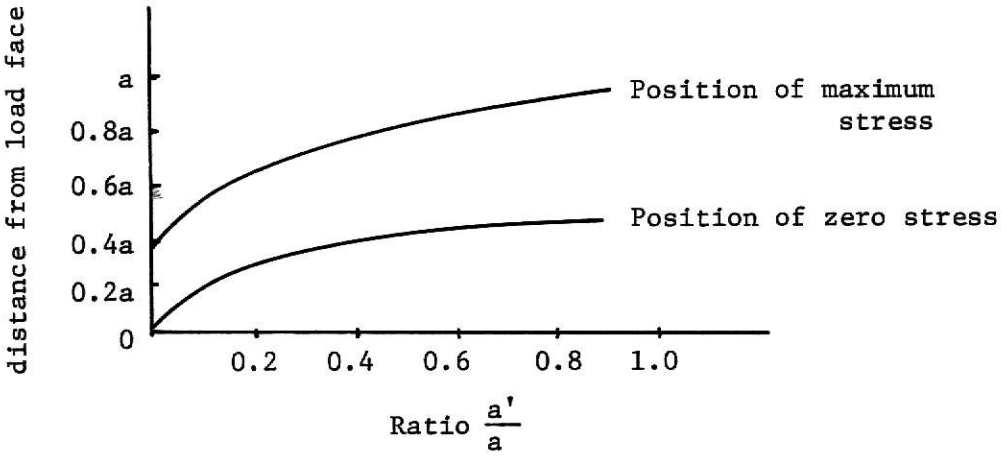

Figure 7b. Position of maximum f_y and f_y=0.

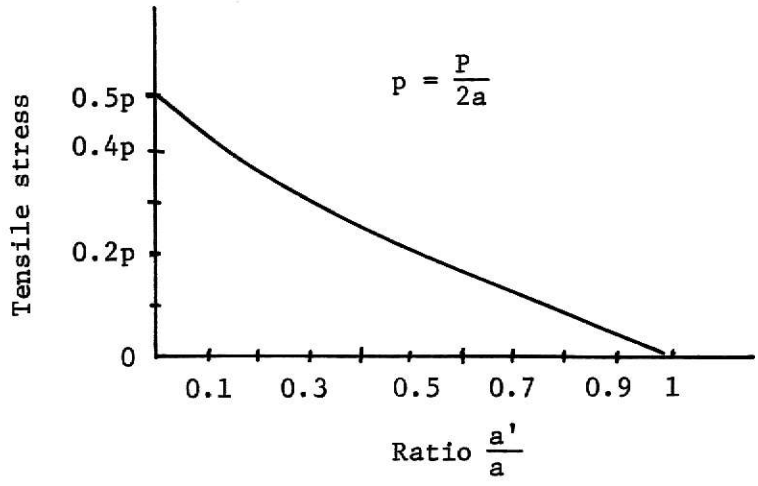

Figure 7c. Maximum value of f_y.

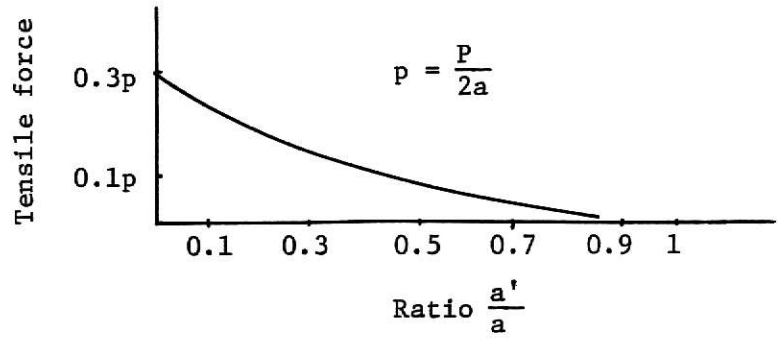

Figure 7d. Value of resultant tensile force.

acting on an infinitesimal area, leading to the indeterminant form $\infty x o$ which must give a concentrated force equal to the total resultant tension (about 0.3P).

Figure 7 shows distribution of f_y on the OX axis; similarly the value of f_y has been obtained for other horizontal planes. The stresses thus obtained can be represented by curves joining points of equal stress value, i. e., by the isobars of f_y, isobars for different values of $\frac{a'}{a}$ are plotted by Guyon, two of which are shown in Fig. 8.

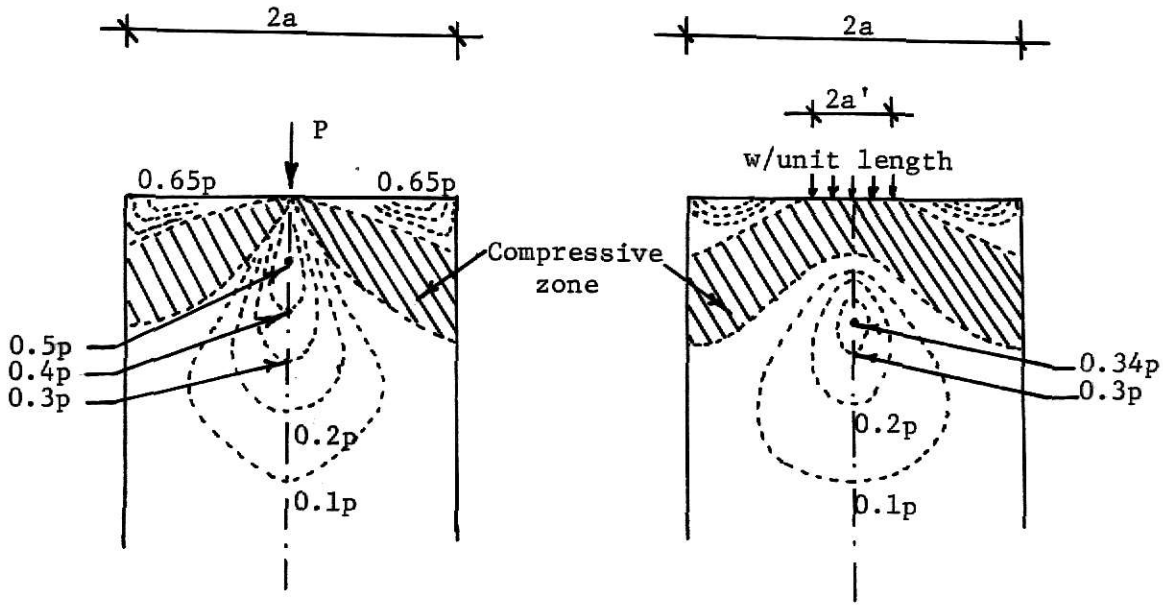

Single concentrated force. Single distributed force.

Figure 8. Isobars of end-blocks.

From this graph it can be found that there are two tensile zones, one in the center of the block along the axis of the load called the "Bursting Zone," the other on the side of the load close to the end surface called the "Spalling Zone." They are separated by a compressive zone. The tensile stress of the spalling zone is high but it acts on a very small area and

hence the total tensile force is small.

Principle of Partitioning. Case of an Axial Prestress Produced by Multiple Symmetrical Forces

The value of the work done in plotting the graph of Fig. 7 will be justified if it can be used more generally with different position of loads.

Consider two axially symmetrical loads $\frac{P}{2}$, displaced a distance of a/2 as shown in Fig. 9. On the axis of the beam introduce a cut "cd" and we will have two beams with a load of P/2 acting on each beam axis. Now the end-block will be of length "a."

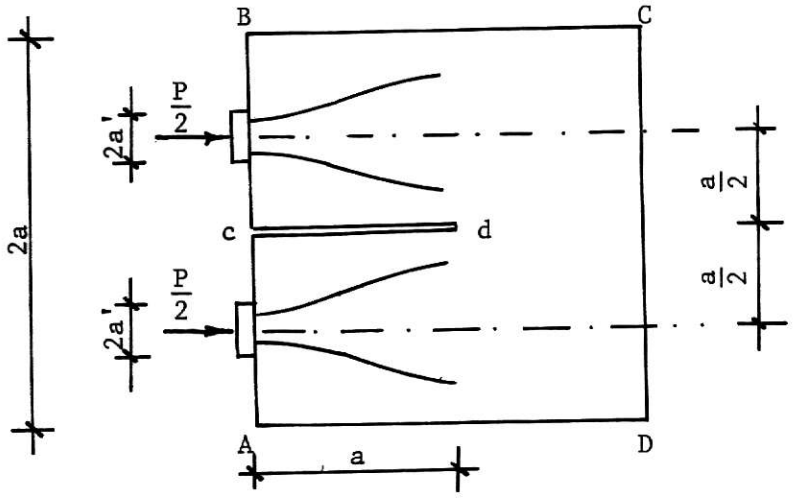

Figure 9. Axially symmetrical loading on end-block.

In this case the ratio of $\frac{a'}{a}$ remains the same as previously but the load becomes one-half as great. The isostatics are similar to those of Fig. 6 but the radius of the curvature will be halved. The stress remains the same, but the length over which this stress is applied is also halved. This indicates that we now need half of the reinforcement.

This can be generalized for number of forces. Thus it can be concluded

that by distributing the force we are shortening the length of the end block. This will help us to place our support nearer to the end. Also, the amount of reinforcement is reduced by $\frac{1}{n}$ times (Fig. 10).

This method of compartmenting and shortening of the end-block is called the principle of partition. This method gives an approximate result, but the approximation is always on the side of safety.

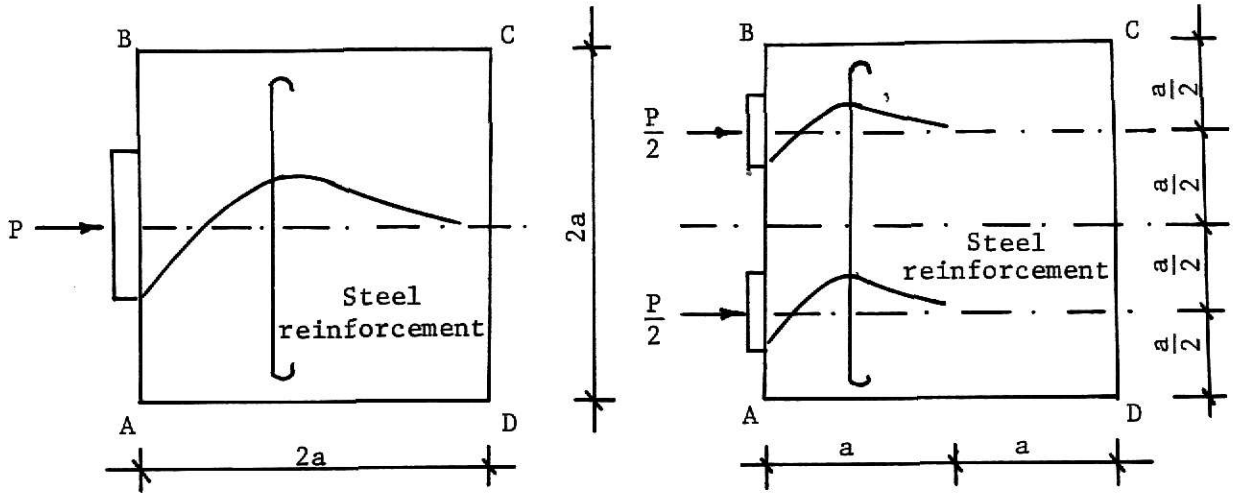

Figure 10. Distribution of f_y of end-block: (a) for single load (b) for two symmetrical load.

Case of Single Eccentric Force: the Symmetrical Prism Method

Figure 11 shows a force P acting with some eccentricity $e = \frac{a}{4}$ and distributed over a height 2a'. The stress diagram at the outer end CD will be trapzoidal. Here Guyon assumes an imaginary symmetrical prism $AB_1C_1D_1$ with a height and length $2a_1$ where a_1 is the distance of force P from the nearest horizontal face of the beam. This will reduce our case to that of a single axial force with some modification in the ratio of $\frac{2a'}{2a_1}$.

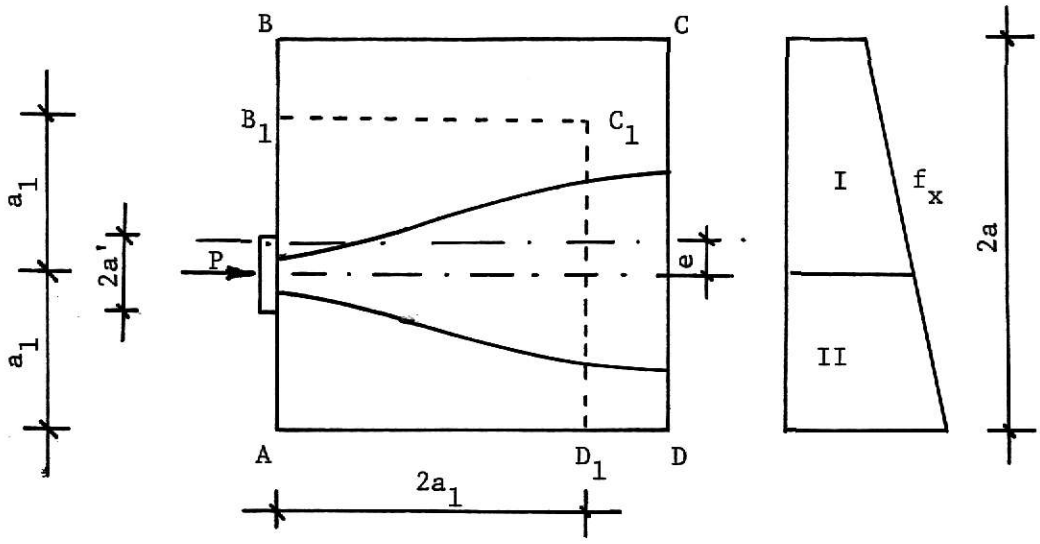

Figure 11. Eccentric loading of end-block.

For example, let $e = \frac{a}{4}$,

Then $a_1 = a - \frac{a}{4} = \frac{3}{4} a$ and $2a_1 = \frac{3}{2} a$

$$p_1 = \frac{P}{2a_1} = \frac{P}{3/2a} = \frac{2}{3} \times \frac{P}{a} = \frac{4}{3} \frac{P}{2a}$$

Therefore $p_1 = \frac{4}{3} p$

The term p_1 is the average compression caused by P on imaginary prism $AB_1C_1D_1$. p is the average compression caused by P on the real prism ABCD. From Fig. 7 the maximum value of $f_y = 0.5P_1 = 0.5 \times \frac{4}{3} P = 0.66 P$ at a distance of $\frac{a_1}{3} = \frac{a}{4}$ on the line of action of the force.

Comparison with the real value from the table for $f_y = 0.54P$ at a distance $\frac{a}{3}$ indicates that the method errs in excess of 22% on the large side. Figure 12 shows the comparison between the approximate and real values. The resultant bursting force calculated by the approximate method is 0.3P, an excess of 7%.

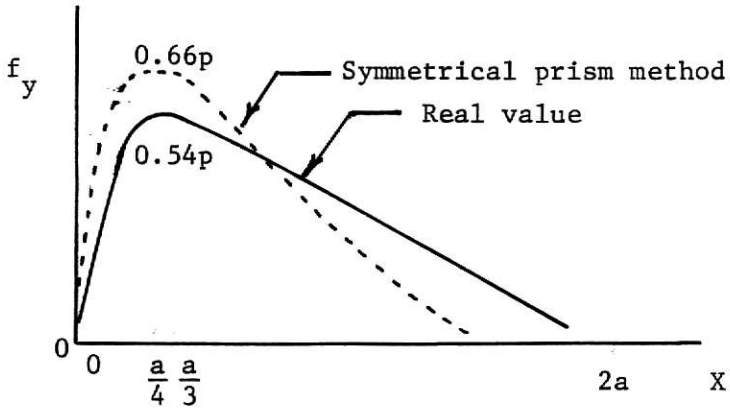

Figure 12. Comparison curve of f_y.

Extension of the Method of Partitioning as well as the Symmetrical Prism Method

Example:

Consider an end-block of depth 20" and width 10" shown in Fig. 13 which we want to prestress to 500 psi on the upper edge and 1000 psi on the lower edge.

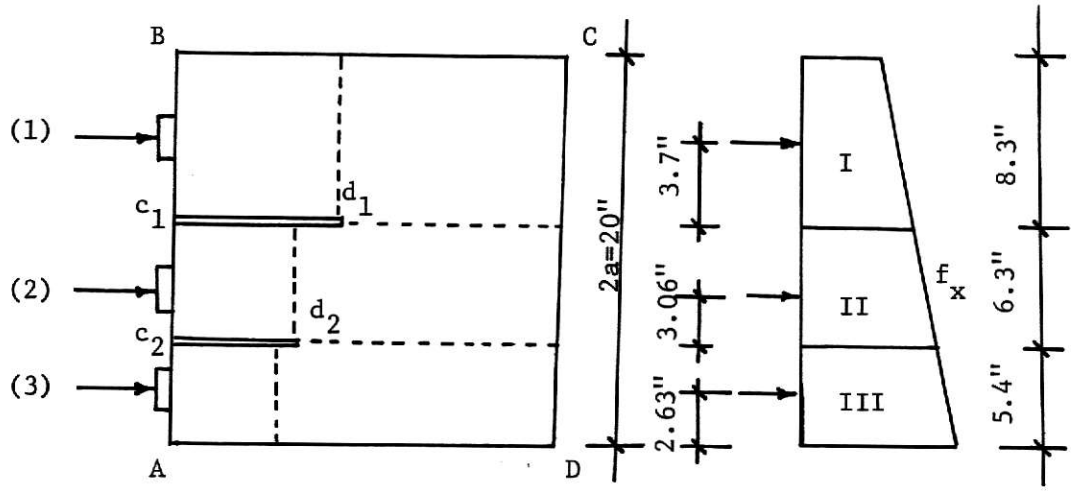

Figure 13. Three eccentric forces on the end-block.

The total pre-stressing force = 10 x 20 x $\frac{500 + 1000}{2}$ = 150 kips. The forces at the end of the beam are so arranged that each lies opposite to the centroid of the corresponding area of the force per unit depth diagram (stress x breadth) beyond the end-block.

Here we will divide 150 k into three forces each of 50 k so that areas of stress trapizids I, II and III are equal. We will introduce imaginary cuts c_1d_1 and c_2d_2 without affecting the state of equilibrium. Now we will apply our symmetrical prism method to find the imaginary prism as we now have to deal with eccentric loads.

Let us suppose 2a' = 3". Then we will end up with the following result as given in Table 1.

TABLE 1. Design of end-blocks.

1	2	3	4	5	6	7	8
Force	Distance of forces from lower face of I, II, III 'a'	Height '2a' of symm. prism	Mean Compressive stress P on symm. prism	$\frac{2a'}{2a}$	Maximum value of f_y from Fig. 7	Distance of max. f_y from AB Fig. 7	Resultant Bursting tension Fig. 7
1	3.7"	7.4"	675 psi	0.405	176 psi	2.92"	6500 lb
2	3.06"	6.12"	816 psi	0.49	180 psi	2.5"	5000 lb
3	2.63"	5.26"	950 psi	0.57	181 psi	2.3"	4500 lb

Column 4 - 1) $\frac{50 \times 1000}{20 \times 7.4}$ = 675 psi

The stress f_y is maximum on the line of action of each force.

Reinforcement

After determining the maximum f_y and its position we will determine the

reinforcement required. Note that a high degree of precision in the calculations would be misleading as the calculations are based on theoretical conditions which are not realized in practice.

Example:

Consider a Freyssinet cone anchorage exerting a force of 3 tons at the center of the compartment of 12" height and 8" breadth and let us investigate the quantity of transverse reinforcement required. Consider the square base of 4" x 4" on which the force is acting uniformly.

Concentration ratio $\frac{2a'}{2a} = \frac{4}{12} = 0.3$

The average compression in the compartment is:

$$p = \frac{30 \times 2240}{8 \times 12} = 700 \text{ psi}$$

From Fig. 7c the maximum tensile stress $f_y = 0.31\ p$

$= 0.31 \times 700$

$= 217$ psi

Max. f_y occurs at $0.72a = 0.72 \times \frac{12}{2} = 4.3"$

And zero f_y is at 1) $0.32a = 0.32 \times \frac{12}{2} = 1.92"$

2) $2a = 12"$

Then an approximate distribution of the stress f_y may be drawn as in Fig. 14. It is triangular with an apex at 4.3" from the bearing surface and points of zero stress at 1.92" and 12", with the maximum value of f_y increased by 10% = 217 x 1.1 = 237 psi.

The area of the triangle $\frac{1}{2} \times (12-1.92) \times 237 = 1200$ lb gives the tensile force per unit breadth, therefore the total force for the 8" breadth = 1200 x 8 = 9600 lb. Now if we consider the allowable tensile stress of concrete as 200 psi then we have to provide steel for the hatched area only.

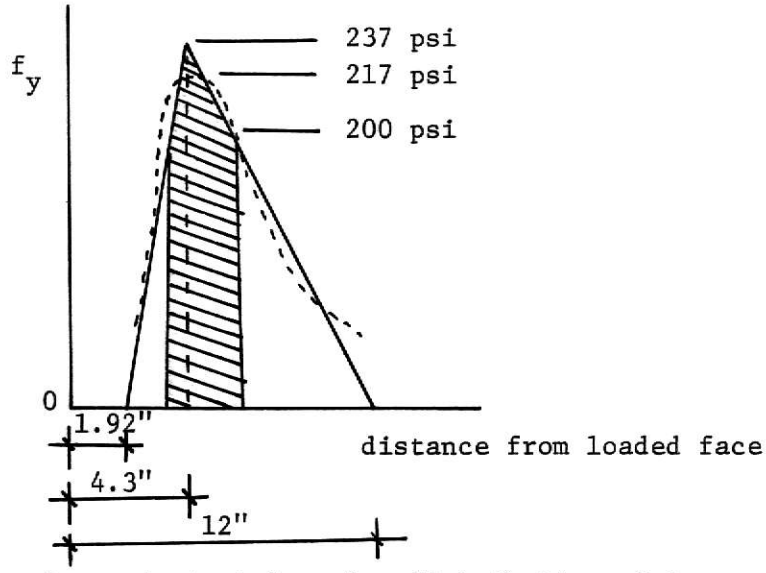

Figure 14. Approximate triangular distribution of f_y.

Let S be the area of the total diagram then the area of the unhatched portion is $Sx(\frac{f_t}{f_y})^2$ and the remaining area = $S\left[1 - (\frac{ft}{f_y})^2\right]$

In our case the force carried by the steel is = $9600\left[1 - (\frac{200}{237})^2\right]$ = 2782 lbs. Steel bars of $\frac{1}{4}$" diameter (A = .049 sq inch) are fitted in the vertical plane parallel to the bearing surface at the point of maximum stress. Therefore, the number of bars required = $\frac{2782}{20000 \times 0.049}$ = 2.84, say 3 bars.

If a Freyssinet cone anchorage is used then we will need reinforcement around the cone for spalling tension in addition to the above reinforcement. Tension of 0.04p may be adopted which will require $\frac{1}{4}$" diameter bars placed as shown in Fig. 15.

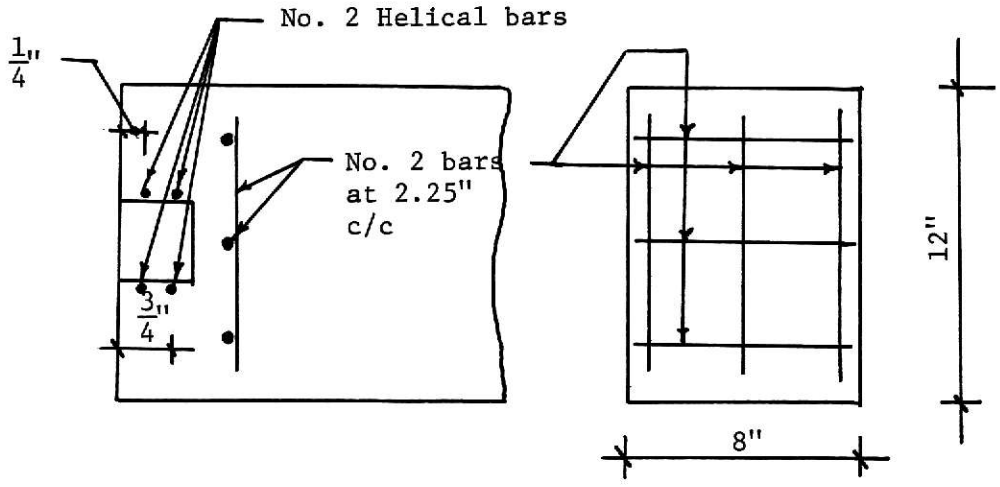

Figure 15. Reinforcement in end-block.

APPROACH OF K. T. SUNDRA RAJA IYENGAR[2][3] ON TWO-DIMENSIONAL ANALYSIS OF END-BLOCKS

K. T. Iyengar found that the two-dimensional analysis given by Magnel, Guyon, Morch and others is not exact and that there is a wide divergence among two-dimensional theories. He undertook to examine critically the many approximate solutions and finally derived the necessary theoretical expressions for two-dimensional problems and also for some specific three-dimensional problems[9]. He used multiple Fourier method to analyze the stress distribution in end-block. His main object was to compare the results of existing approximate methods to a more exact method derived by him.

The assumptions made by him were: 1) the problem permits two-dimensional analysis; 2) the effect of the cable ducts is ignored.

He considered a semi-infinite strip with loads on narrow ends. Unlike other authors he did not assume that the stress induced by the cables would become normal, i. e., the stresses are almost entirely longitudinal, in a distance equal to the beam depth, since he did not assume that St. Venant's principle applied.

Since there are normal as well as oblique forces acting at the end of the beam, he considered four general cases[2]:

(1) Normal loading, symmetrical about x axis.

(2) Normal loading, antisymmetrical about x axis.

(3) Tangential loading, symmetrical about x axis.

(4) Tangential loading, antisymmetrical about x axis.

Note: All the equations given below are taken from reference (2).

Case I. Normal symmetrical force.

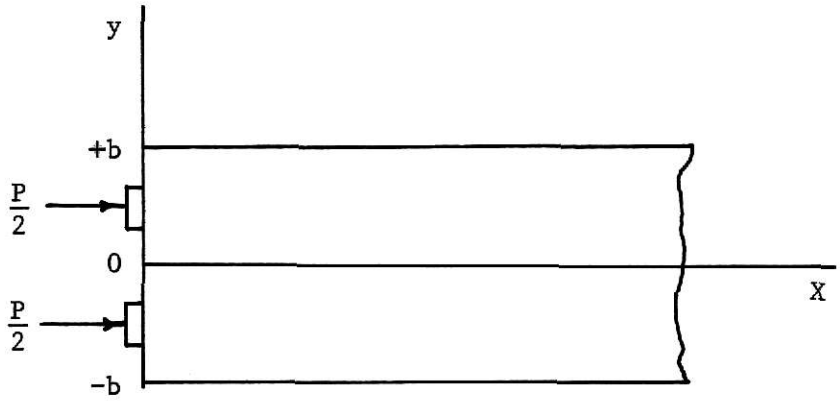

Figure 16. End-block subjected to normal symmetrical forces.

When $x = 0 \quad f_x = - f_1(y)$.

at $x = \infty \quad f_x = - \frac{P}{2b}$

Hence $f_1(y)$ can be expanded in fourier series as follows:

$$f_1(y) = \frac{P}{2b} + \sum_{m=1,2,3}^{\infty} I_m \cos \frac{m\pi x}{b}$$

where

$$I_m = \frac{1}{b} \int_{-b}^{+b} f_1(y) \cos \frac{m\pi x}{b} \, dy \qquad (3)$$

The stress components are given by

$$f_x = - \frac{P}{2b} - \sum_{m=1,2,3} A_m \left[\cos \frac{m\pi x}{b} \left(1 + \frac{m\pi y}{b}\right) e^{-(m\pi x/b)} - m(-1)^m F_m \right]$$

$$f_y = \sum_{m=1,2,3} A_m \left[\cos \frac{m\pi y}{b} \left(-1 + \frac{m\pi y}{b}\right) e^{-(m\pi x/b)} - m(-1)^m H_m \right]$$

$$t = - \sum_{m=1,2,3} A_m \left[\sin \frac{m\pi y}{b} \frac{m\pi x}{b} e^{-(m\pi x/b)} - m(-1)^m S_m \right] \qquad (4)$$

Where

$$F_m = 4b^3 \int_0^\infty \frac{[\alpha y \sinh \alpha y + (1 - \alpha b \coth \alpha b) \cosh \alpha y]}{[(\alpha b)^2 + (m\pi^2)]^2 \left[\cosh \alpha b + \frac{\alpha b}{\sinh \alpha b}\right]} \alpha^2 \cos \alpha x d\alpha .$$

$$H_m = 4b^3 \int_0^\infty \frac{[\alpha y \sinh \alpha y - (1 + \alpha b \coth \alpha b) \cosh \alpha y]}{[(\alpha b)^2 + (m\pi^2)]^2 \left[\cosh \alpha b + \frac{\alpha b}{\sinh \alpha b}\right]} \alpha^2 \cos \alpha x d\alpha .$$

$$S_m = 4b^3 \int_0^\infty \frac{[\alpha y \cosh \alpha y - \alpha b \coth \alpha b \sinh \alpha y]}{[(\alpha b)^2 + (m\pi^2)]^2 \left[\cosh \alpha b + \frac{\alpha b}{\sinh \alpha b}\right]} \alpha^2 \sin \alpha x d\alpha . \quad (5)$$

And "A_m" are given by the set of simultaneous equations

$$A_m = I_m + 16\pi^2 m^2 \sum_{r=1,2,3\ldots} (-1)^{r+m} r A_r k(r,m) \quad (6)$$

with

$$K(r,m) = \int_0^\infty \frac{x^3 \tanh x}{\left[1 + \frac{2x}{\sinh 2x}\right] (x^2 + r^2\pi^2)^2 (x^2 + m^2\pi^2)^2} dx .$$

Equation (6) can be put in the form

$$A_m (1 - p_{mm}) = I_m + \sum_{r=1,2,3\ldots} p_{mr} A_r \quad (7)$$

where $m \neq r$

and $p_{mr} = 16\pi^2 m^2 r (-1)^{r+m} K(r,m)$

The equation (7) can be written as

$$A_m = \sum_{r=1,2,3\ldots} M_{mr} I_r \quad (8)$$

where M_{mr} is the inverse matrix of the coefficients of A_m in Eq. (7), so

knowing "A_m" the stresses can be calculated from Eq. (4). The stress components in Eq. 4 satisfy all the equations of elasticity, that is, equilibrium, compatibility and boundary conditions.

Case 2. Normal antisymmetrical forces (see Fig. 17).

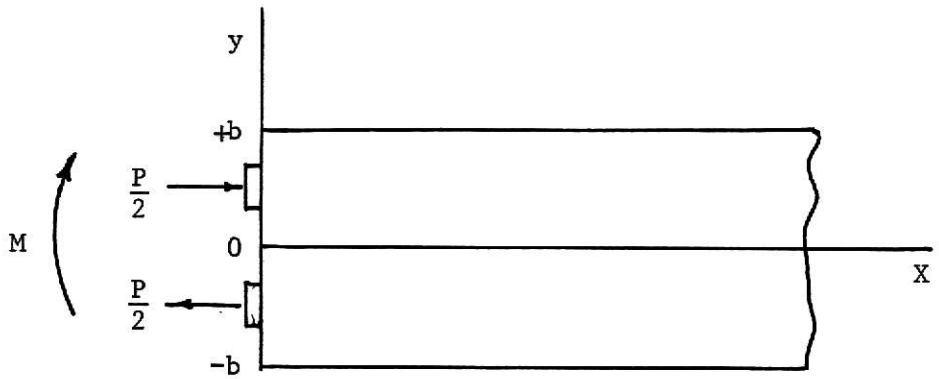

Figure 17. End-block subjected to normal antisymmetrical forces.

In this case

$$\text{at } x = 0 \quad f_x = -f_2(y)$$

$$\text{at } x = \infty \quad f_x = \frac{-3my}{2b^3}$$

where

$$m = \int_{-b}^{+b} f_2(y)\, y\, dy \ .$$

The stress components are

$$f_x = -\frac{3my}{2b^3} - \sum_{n=1,3,5\ldots} B_n \left[\sin \frac{n\pi y}{2b} \left(1 + \frac{n\pi x}{2b}\right) e^{-(m\pi x/2b)} - \frac{n}{2}(-1)^{(n-1)/2} G_n \right]$$

$$f_y = \sum_{n=1,3,5\ldots} B_n \left[\sin \frac{n\pi y}{2b} \left(-1 + \frac{n\pi x}{2b}\right) e^{-(n\pi x/2b)} - \frac{n}{2}(-1)^{(n-1)/2} R_n \right]$$

$$t = \sum_{n=1,3,5\ldots} B_n \left[\cos \frac{n\pi y}{2b} \frac{n\pi x}{2b} e^{-(n\pi x/2b)} + \frac{n}{2}(-1)^{(n-1)/2} T_n \right] \qquad (9)$$

Where

$$G_n = 4b^3 \int_0^\infty \frac{[\alpha y \cosh \alpha y + (1 - \alpha b \tanh \alpha b) \sinh \alpha y]}{[(\alpha b)^2 + (\frac{n\pi}{2})^2]^2 \left[\sinh \alpha b - \frac{\alpha b}{\cosh \alpha b}\right]} \alpha^2 \cos \alpha x d\alpha .$$

$$R_n = 4b^3 \int_0^\infty \frac{[\alpha y \cosh \alpha y - (1 + \alpha b \tanh \alpha b) \sinh \alpha y]}{[(\alpha b)^2 + (\frac{n\pi}{2})^2]^2 \left[\sinh \alpha b - \frac{\alpha b}{\cosh \alpha b}\right]} \alpha^2 \cos \alpha x d\alpha .$$

$$T_n = 4b^3 \int_0^\infty \frac{[\alpha y \sinh \alpha y - \alpha b \tanh \alpha b \cosh \alpha y]}{[(\alpha b)^2 + (\frac{n\pi}{2})^2]^2 \left[\sinh \alpha b - \frac{\alpha b}{\cosh \alpha b}\right]} \alpha^2 \sin \alpha x d\alpha .$$

(10)

and "B_n" are given by

$$B_n = I_n + 16\pi^2 (1/2n)^2 \sum_{s=1,3,5\ldots} (-1)^{(s+n-2)/2} \, 1/2s \, B_s \, L(s,n) \qquad n=1,3,5\ldots \qquad (11)$$

In Eq. (11)

$$I_n = \frac{1}{b} \int_{-b}^{+b} f_2(y) - \frac{3my}{2b^3} \sin \frac{n\pi y}{2b} dy$$

and

$$L(s,n) = \int_0^\infty \frac{x^3 \coth x \, dx}{\left[1 - \frac{2x}{\sinh 2x}\right][x^2 + (\frac{s\pi}{2})^2]^2 [x^2 + (\frac{n\pi}{2})^2]^2}$$

The solution of Eq. (11) can be written as

$$B_n = \sum_{s=1,2,3\ldots} N_{ns} I_s . \qquad (12)$$

Where "N_{ns}" is the inverse matrix of the coefficient of "B_n" in the linear Eq. (11).

Case III. Tangential symmetrical forces (see Fig. 18).

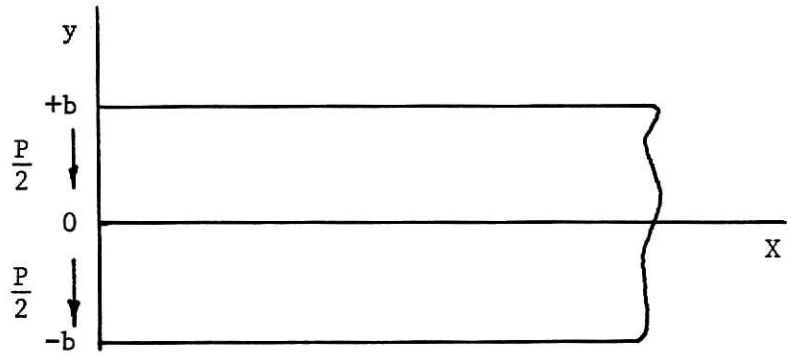

Figure 18. End-block subjected to tangential symmetrical forces.

In this case

$$t = g_1(y) \quad \text{at} \quad x = 0$$

and according to St. Venant's principle

$$t = \frac{3P}{4b}\left(1 - \frac{y^2}{b^2}\right) \quad \text{at} \quad x = \infty$$

where

$$P = \int_{-b}^{+b} g_1(y)\, dy$$

The stress components are

$$f_x = \frac{3Pxy}{2b^3} - \sum_{m=1,2,3\ldots} A_m' \sin\left[\frac{m\pi y}{b}\frac{m\pi x}{b} e^{-(m\pi x/b)} + m(-1)^m F_m'\right]$$

$$f_y = \sum_{m=1,2,3\ldots} A_m' \left[\sin\frac{m\pi y}{b}\left(\frac{m\pi x}{b} - 2\right) e^{-(m\pi x/b)} + m(-1)^m H_m'\right]$$

$$t = \frac{3P}{4b}\left(1 - \frac{y^2}{b^2}\right) - \sum_{m=1,2,3\ldots} A_m' \left[\cos \frac{m\pi y}{b}\left(1 - \frac{m\pi x}{b}\right) e^{-(m\pi x/b)} - m(-1)^m S_m'\right]$$

(13)

Where

$$F_m' = 4b^3 \int_0^\infty \frac{[\alpha y \cosh \alpha y + (2 - \alpha b \coth \alpha b) \sinh \alpha y]}{[(\alpha b)^2 + (m\pi)^2]^2 \left[\cosh \alpha b - \frac{\alpha b}{\sinh \alpha b}\right]} \alpha^2 \sin \alpha x d\alpha .$$

$$H_m' = 4b^3 \int_0^\infty \frac{[\alpha y \cosh \alpha y - \alpha b \coth \alpha b \sinh \alpha y]}{[(\alpha b)^2 + (m\pi)^2]^2 \left[\cosh \alpha b - \frac{\alpha b}{\sinh \alpha b}\right]} \alpha^2 \sin \alpha x d\alpha .$$

$$S_m' = 4b^3 \int_0^\infty \frac{[\alpha y \sinh \alpha y + (1 - \alpha b \coth \alpha b) \cosh \alpha y]}{[(\alpha b)^2 + (m\pi)^2]^2 \left[\cosh \alpha b - \frac{\alpha b}{\sinh \alpha b}\right]} \alpha^2 \cos \alpha x d\alpha .$$

(14)

A_m' are given by

$$A_{m=1,2,3\ldots}' = -I_m' + 16\pi^2 m^2 \sum_{r=1,2,3\ldots} (-1)^{r+m} r A_r' K'(r,m)$$

(15)

In Eq. (15)

$$I_m' = \frac{1}{b} \int_{-b}^{+b} g_1(y) - \frac{3P}{4b}\left(1 - \frac{y^2}{b^2}\right) \cos \frac{m\pi y}{b} dy .$$

and

$$K'(r,m) = \int_0^\infty \frac{x^3 \tanh x \, dx}{\left[1 - \frac{2x}{\sinh 2x}\right](x^2 + r^2\pi^2)^2 (x^2 + m^2\pi^2)^2}$$

The solution of Eq. (15) is given by

$$A_m' = \sum_{r=1,2,3\ldots} M'_{mr} I_r'$$

(16)

Where M'_{mr} is the coefficient matrix of the coefficients of A_m' in Eq. (15).

Case IV. Tangential antisymmetrical force (see Fig. 19).

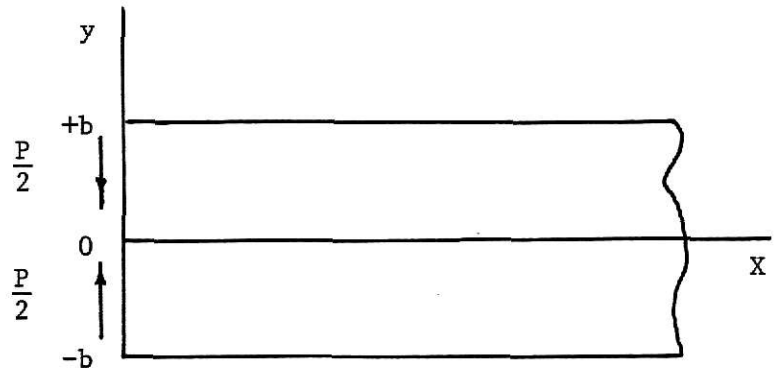

Figure 19. End-block subjected to tangential antisymmetrical forces.

Here

$$x = 0 \quad t = g_2(y)$$

$$x = \infty \quad t = 0$$

$$g_2(y) = \sum_{n=1,3,5\ldots} I_n' \sin \frac{n\pi x}{2b}$$

The stress components are

$$f_x = -\sum_{n=1,3,5\ldots} B_n' \left[\cos \frac{n\pi y}{2b} \frac{n\pi x}{2b} e^{-(n\pi x/2b)} - \frac{n}{2}(-1)^{(n-1)/2} G_n'\right]$$

$$f_y = \sum_{n=1,3,5\ldots} B_n' \left[\cos \frac{n\pi x}{2b}\left(\frac{n\pi y}{2b} - 2\right) e^{-(n\pi x/2b)} - \frac{n}{2}(-1)^{(n-1)/2} R_n'\right]$$

$$t = \sum_{n=1,3,5\ldots} B_n' \left[\sin \frac{n\pi x}{2b}\left(1 - \frac{n\pi y}{2b}\right) e^{-(n\pi x/2b)} - \frac{n}{2}(-1)^{(n-1)/2} T_n'\right] \qquad (17)$$

where

$$G_n' = 4b^3 \int_0^\infty \frac{[\alpha y \sinh \alpha y + (2 - \alpha b \tanh \alpha b) \cosh \alpha y]}{\left[(\alpha b)^2 + \left(\frac{n\pi}{2}\right)^2\right]^2 \left[\sinh \alpha b + \frac{\alpha b}{\cosh \alpha b}\right]} \alpha^2 \sin \alpha x d\alpha \ .$$

$$R_m' = 4b^3 \int_0^\infty \frac{[\alpha y \sinh \alpha y - \alpha b \tanh \alpha b \cosh \alpha y]}{\left[(\alpha b)^2 + (\frac{n\pi}{2})^2\right]^2 \left[\sinh \alpha b + \frac{\alpha b}{\cosh \alpha b}\right]} \alpha^2 \sin \alpha x d\alpha .$$

$$T_m' = 4b^3 \int_0^\infty \frac{[\alpha y \cosh \alpha y + (1 - \alpha b \tanh \alpha b) \sinh \alpha y]}{\left[(\alpha b)^2 + (\frac{n\pi}{2})^2\right]^2 \left[\sinh \alpha b + \frac{\alpha b}{\cosh \alpha b}\right]} \alpha^2 \cos \alpha x d\alpha . \quad (18)$$

B_n' are given by

$$B_{n\ n=1,3,5\ldots}' = I_n' + 16\pi^2 (1/2n)^2 \sum_{s=1,3,5\ldots} (-1)^{(s+n-2)/2}\ 1/2s\ B_s' L'(s,n) \quad (19)$$

where

$$I_n' = \frac{1}{b} \int_{-b}^{+b} g_2(y) \sin \frac{n\pi y}{2b} dy$$

and

$$L'(s,n) = \int_0^\infty \frac{x^3 \coth x\, dx}{\left[1 + \frac{2x}{\sinh 2x}\right]\left[x^2 + (\frac{s\pi}{2})^2\right]^2 \left[x^2 + (\frac{n\pi}{2})^2\right]^2}$$

The solution of Eq. (19) is

$$B_n' = \sum_{s=1,3,5\ldots} N_{ns}'\ I_s' \quad (20)$$

Where N'_{ns} is inverse matrix of the coefficient of B_n' in Eq. (19).

The author of the reference has prepared tables containing values of the inverse matrices M_{mr}, M'_{mr}, N_{ns}, N'_{ns} in Eqs. (8), (12), (16), and (20), and values of coefficients for calculating f_x, f_y, and t stress components for the first two cases in his Ph.D. thesis, but due to nonavailability of that book it cannot be reproduced here.

The graphs of distribution of transverse stress along the axis, and positions of maximum and zero f_y are shown in Fig. 20[(2)]. These graphs will be used to solve the numerical example, and are drawn for single axial load with different sizes of bearing plates.

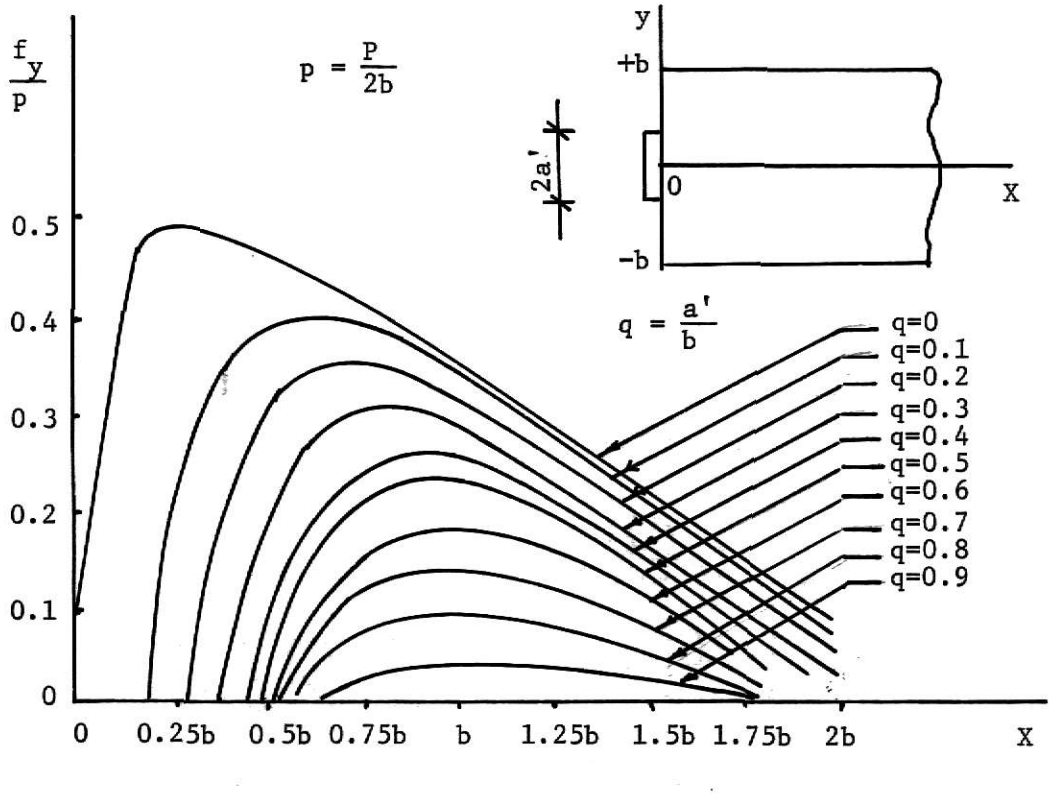

Figure 20a. Distribution of transverse tensile stress along load axis y = 0, for different values of q.

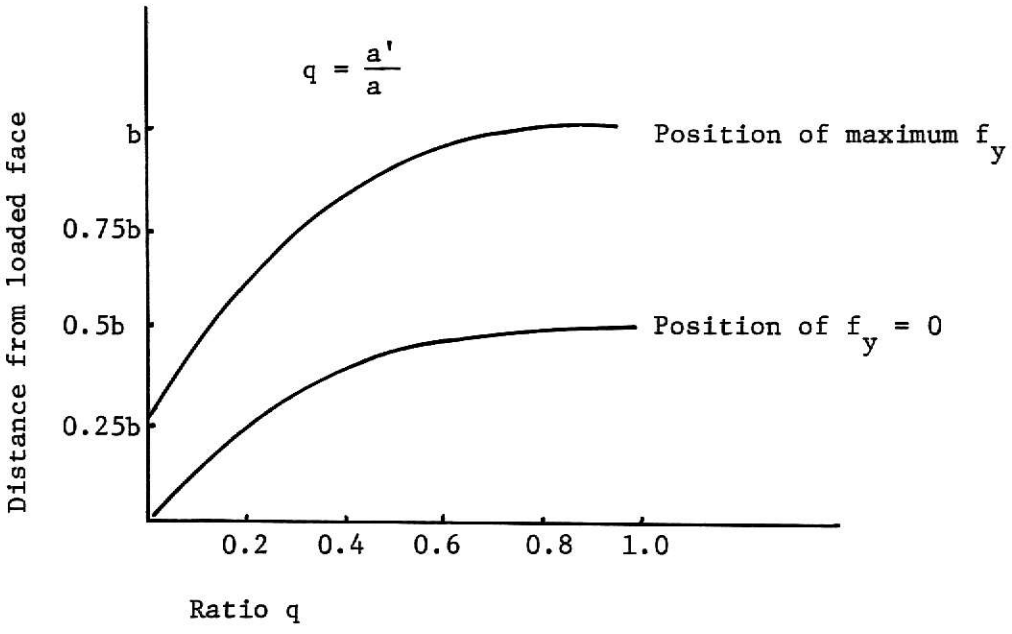

Figure 20b. Position of maximum f_y and $f_y = 0$.

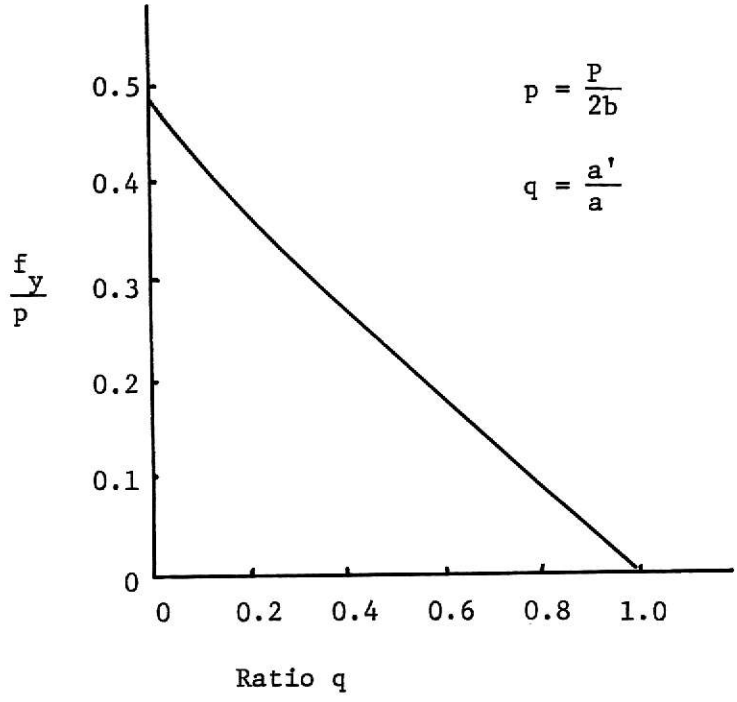

Figure 20c. Maximum value of f_y.

APPROACH OF R. J. LENSCHOW AND M. A. SOZEN[4]

PHYSICAL ANALOG METHOD

The authors, R. J. Lenschow and M. A. Sozen, have tried to develop a new method to find out stresses in end-blocks. Their main object was to find a method which can be used in design to investigate many different conditions without the necessity of laborious solutions.

The term bursting stress (referred to as bursting zone by Guyon) is the tensile stress across the axis of the applied load, e. g., section BB in Fig. 21. Spalling stress (spalling zone) is the tensile stress across any other longitudinal section, e. g., section AA in Fig. 21.

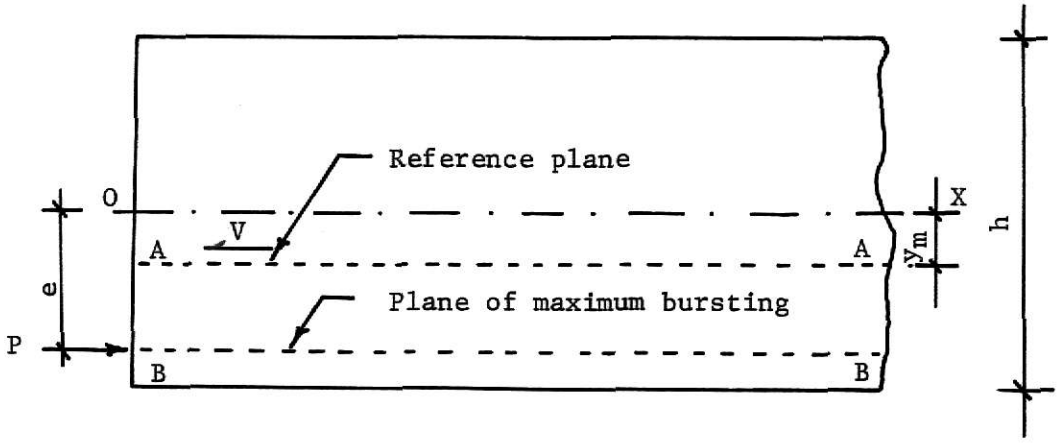

Figure 21. Position of plane of maximum bursting stress and reference plane in end-block.

The authors assume cuts across section AA and BB, and fictitious springs have been introduced as shown in Fig. 22 to simulate the distribution of bursting and spalling stresses.

Section AA is considered as a reference plane. The beam in Fig. 21 is

represented by two beams in Fig. 22. The loading in Fig. 22a is symmetrical about the beam centroid as are the cuts introduced, one of these being at the reference plane. Fictitious springs, representing the concrete, resist the deflection of the outer part of the beam. The loading in Fig. 22b is adjusted so that the two parts of the cut beam have the same curvature; the fictitious springs are not required.

Loading in Fig. 22 must be equal to loading in Fig. 21. For this

$$P_0 - P_2 = 0 \qquad (21)$$

$$P_0 + P_1 = P \qquad (22)$$

$$V_0 + V_1 = V \qquad (23)$$

where V is the shear force that would exist along the reference plane.

The bending moment can be written as $M_0 = -P_0 e_1 - V_0 e_2$ (24)

To make the bottom portion of the analog in Fig. 22b conform to the

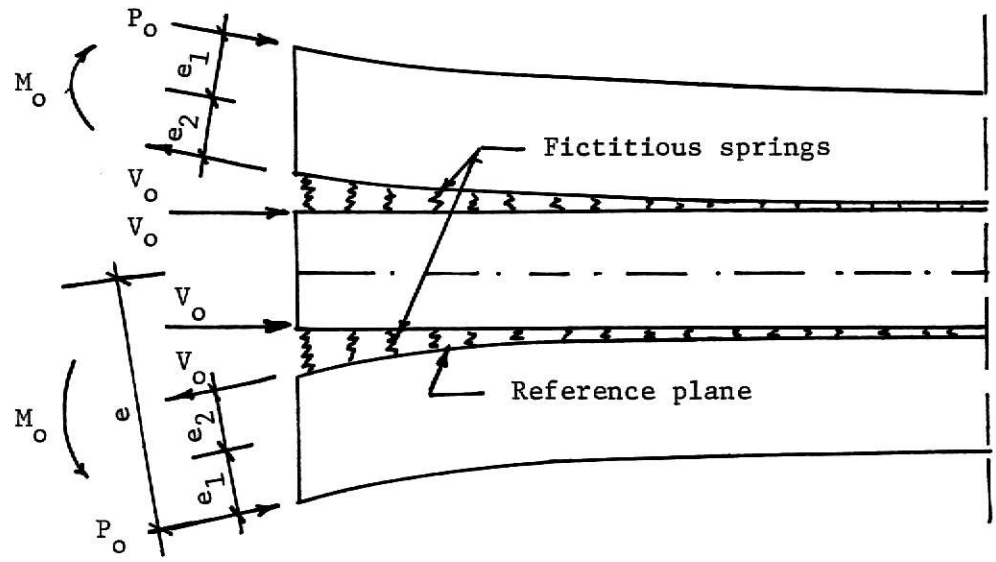

Figure 22a. The physical analog.

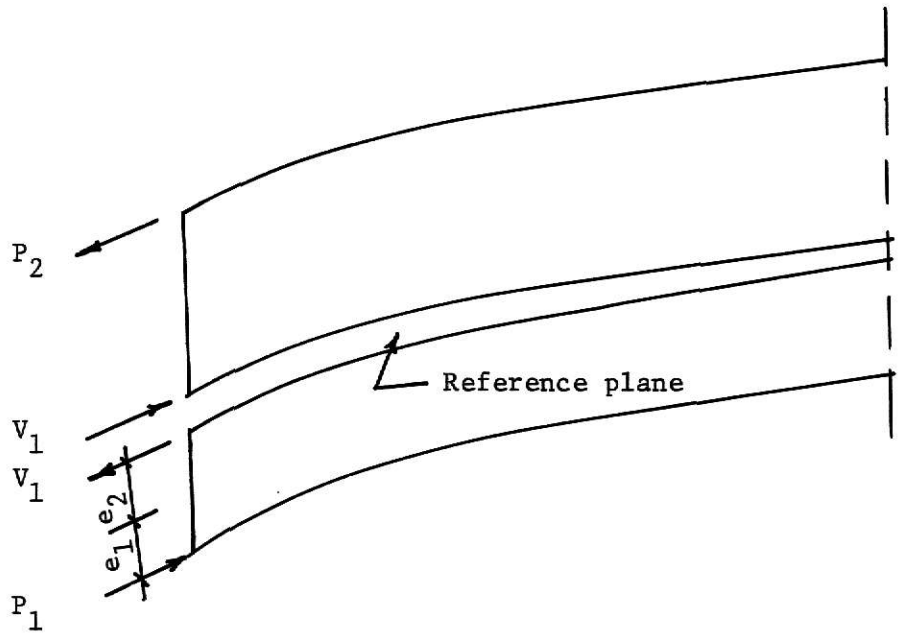

Figure 22b. The physical analog.

curvature of the whole beam

$$\frac{P_1 e_1 + V_1 e_2}{E_c I_b} = \frac{Pe}{E_c I} \qquad (25)$$

Where

I_b = Moment of inertia of the portion below the reference plane

I = Moment of inertia of the whole beam

E_c = Modulus of elasticity of concrete

From Eq. 25

$$P_1 e_1 + V_1 e_2 = Pe \frac{I_b}{I} \qquad (25b)$$

From Eq. 21 to 23

$$P_0e_1 + V_0e_2 = Pe_1 - P_1e_1 + Ve_2 - V_1e_2$$

$$= Pe_1 + Ve_2 - (Pe_1 + V_1e_2)$$

Substitute in (25b)

$$= Pe_1 + Ve_2 - Pe\frac{I_b}{I} \qquad (26)$$

From (24) $$M_o = M_p + M_v - M_t\frac{I_b}{I} \qquad (27)$$

where M_p and M_v refer to the moments acting on the portion of the analog below the reference plane and M_t is the moment on the whole beam.

The authors of the reference now consider the portion of the beam below the reference plane as a beam on an elastic foundation. The stresses in the fictitious spring should indicate the transverse stresses.

Then the spring force F per unit length of the beam is

$$F = ky \qquad (28)$$

where

k = spring constant

y = deflection of the spring

The deflection of a beam on elastic foundation, corresponding to the lower portion of the physical analog can be expressed as

$$y = e^{-ax}(C_3 \cos gx + C_4 \sin gx)^* \qquad (29)$$

and $$f_y = \frac{F}{b} = \frac{k}{b}e^{-ax}(C_3 \cos gx + C_4 \sin gx) \qquad (30)$$

where

x is the distance from the beam end.

---

*Detailed explanation is given in reference (8), pages 141-145.

and values of g are constant and related to the stiffness of the beam and springs.

C_3 and C_4 are constant and determined by the boundary conditions.

b is the width of the beam at the reference plane.

Maximum Spalling and Bursting Stresses in Uncracked Beam

The authors of the reference here give the expressions for maximum spalling and bursting stresses. The maximum spalling stress along the reference plane, i. e., section AA in Fig. 21 at x = 0 is

$$f_{ys} = -\frac{M_o}{b}\sqrt{\frac{k}{E_c I_b}} \qquad (31)$$

The general solution for maximum bursting stress becomes too complex and hence the authors have given a close approximation for maximum bursting stress caused by a concentrated load.

$$f_{ybc} = \frac{1}{2\sqrt{6}}\,\frac{M_o}{b}\sqrt{\frac{k}{E_c I_b}} \qquad (32)$$

f_{ybc} = bursting stress due to concentrated load.

The spring constant k is given by

$$k = b_{eq} E_c / C \qquad (33)$$

where C is the distance from the reference plane to the centroid of the lower portion of physical analog; b_{eq} is the imaginary width, equivalent to the real geometric form with respect to the spring constant. (The term b_{eq} may be taken as the average effective thickness over distance C.)

For rectangular sections b_{eq} = b and c = 1/2 h_b where h_b is the height of the section below the reference plane.

On substituting for b_{eq} and C the expression for maximum spalling stress simplifies to

$$f_{ys} = - M_o \frac{2\sqrt{6}}{bh_b^2} \qquad (34)$$

and maximum bursting stress simplifies to

$$f_{ybc} = M_o \frac{1}{bh_b^2} \qquad (35)$$

It is necessary to find out the reference plane on which the spalling stress is maximum. The authors have given simple approximate expression

$$y_m = \frac{1}{3} (7e - 2h) \qquad (36)$$

where

y_m = the distance of reference plane from the mid-height of the beam

e = the eccentricity of load

The load is mostly applied through the bearing plate and hence it does not remain concentrated but becomes distributed. The authors have studied the effect of distribution with the use of analogs and have plotted a graph, Fig. 23, for the case in which the centroid of the load coincides with the centroid of the section. For comparison Guyon's result is also plotted.

The expressions for the case where the centroid of the load does not coincide with the centroid of the beam is given by

$$\frac{f_{yb}}{f_{ybc}} = 1 - \frac{bt}{A} (3 - 4 \frac{A_b}{A}) \qquad (37)$$

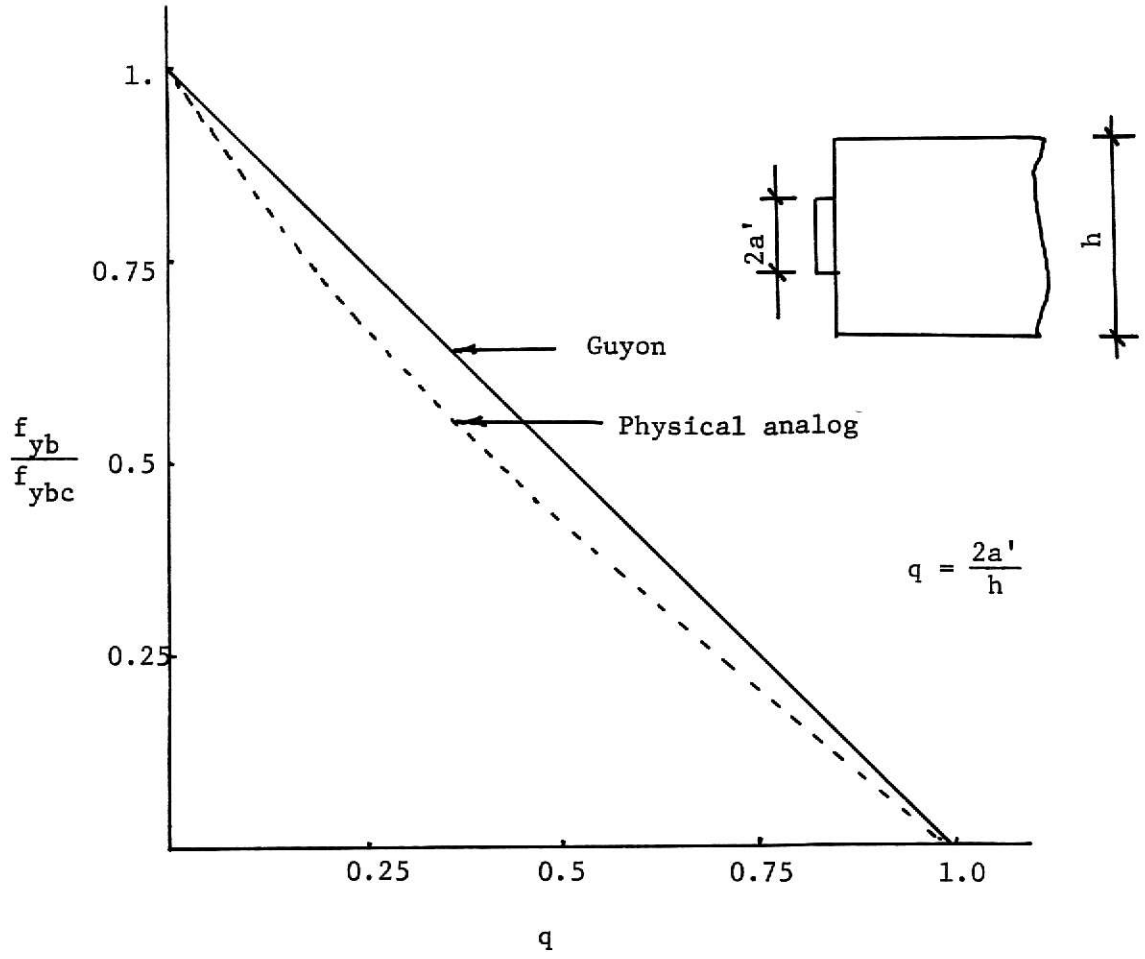

Figure 23. Influence of the distribution of the load on bursting stress.

where

A_b = area of the section below the reference plane

A = area of the whole cross section.

For the rectangular section

$$\frac{bt}{A} = \frac{t}{h} \quad \text{and} \quad \frac{A_b}{A} = \frac{h_b}{h}$$

and

$$\frac{f_{yb}}{f_{ybc}} = 1 - \frac{t}{h}\left(3 - 4\,\frac{h_b}{h}\right) \qquad (37a)$$

Reinforcement to Restrain Spalling Cracks

The force in the reinforcement is related to the crack opening through its bond-slip characteristics. The authors of the reference have given a simple expression to determine the force in the reinforcement after neglecting the tensile strength of concrete as

$$F_o = -M_o \sqrt{\frac{1}{E_c I_b \frac{9\gamma}{A_b G} - \frac{3W}{M_o}}} \qquad (38)$$

where

W = the width of spalling crack at the reinforcement location

γ = the shape factor usually used for determination of shear deflection

G = shear modulus = $\frac{E_c}{2(1+u)}$

u = the possion's ratio.

If the tensile strength of concrete is considered then F_o will be modified to F_1 as

$$F_1 = F_o \left(1 - \frac{E_c I_b}{k} \frac{bf_t}{M_o}\right)^2 \qquad (39)$$

where

f_t is the tensile strength of concrete.

Reinforcement to Prevent Bursting Cracks

The expression for the force in the reinforcement is given by

$$f_o = \frac{M_o}{h_b^2} \left(1 - \frac{f_t}{f_{yb}}\right)$$

where f_{yb} is calculated from Eq. (37).

The position of the transverse reinforcement is very important. The stirrups very close to and very far from the loaded face have little effect. To provide a large number of light stirrups at close intervals is a good solution according to the authors. The stress in the transverse reinforcement should be limited to that attained at the time of cracking of the concrete.

Finally, the authors compare their results with those of Guyon by graphs as shown in Figs. 24 and 25.

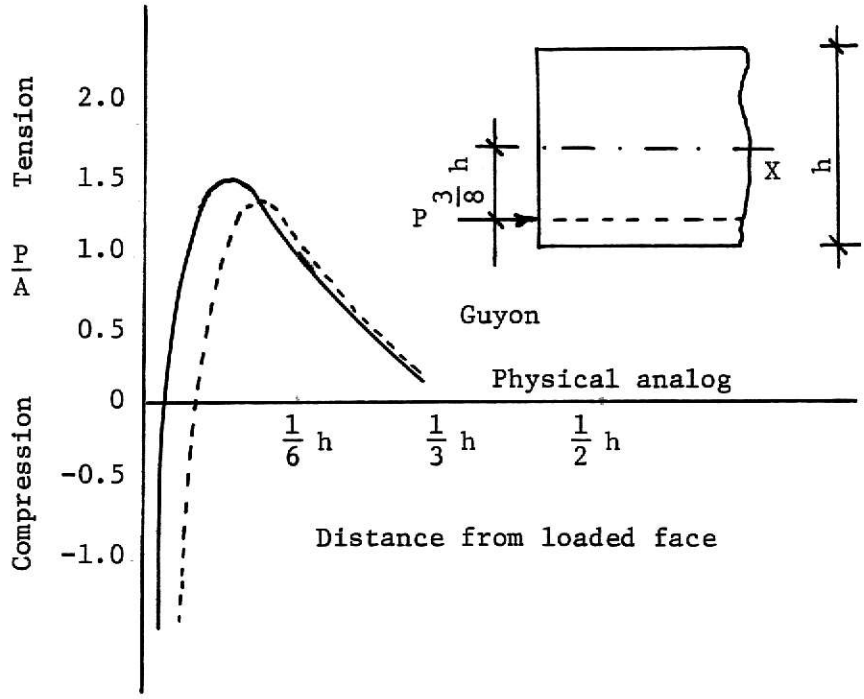

Figure 24. Comparison of bursting stresses under an eccentric load.

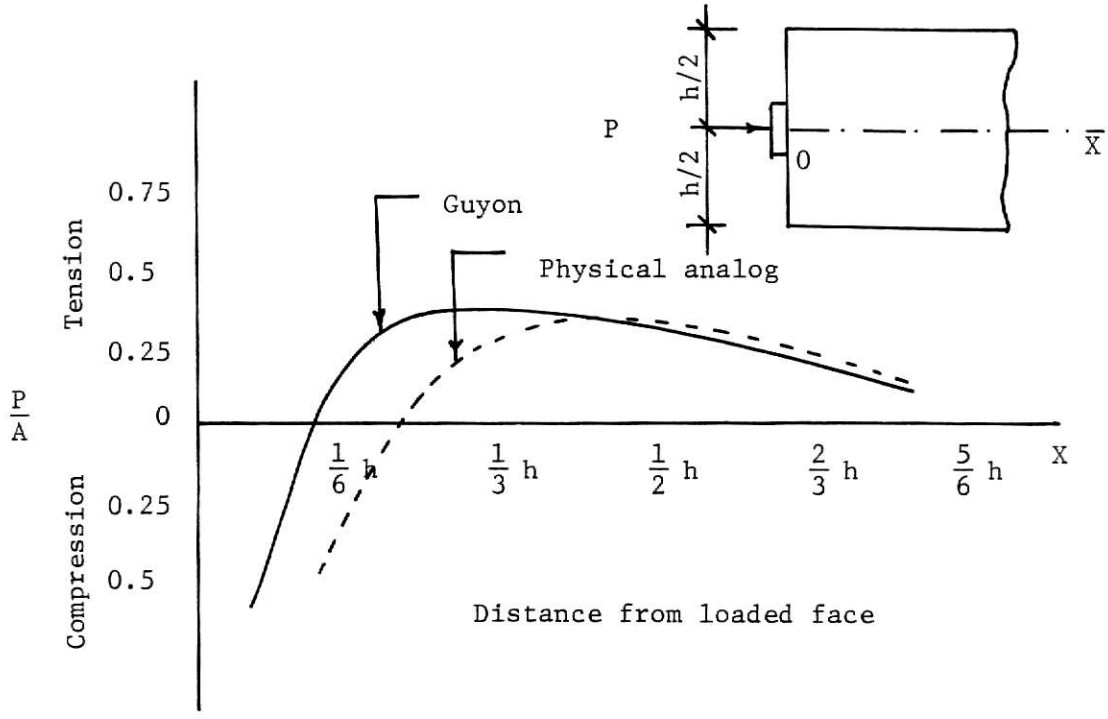

Figure 25. Comparison of bursting stress under a symmetrical load.

EXAMPLES

Numerical examples are solved here with the view of comparing the results obtained by the three foregoing authors.

Example 1

To find the maximum bursting stress and spalling stress and their positions (wherever possible) with the following data.

1) height of block 20" = h = 2a

2) width of block 9"

3) single tendon with prestressing force of 100 kips

The stresses are to be calculated with load eccentricity of 0, $\frac{h}{8}$, $\frac{h}{4}$, $\frac{3}{8}$ h for the case; a) for concentrated force, b) with bearing plate of 3" x 3" size.

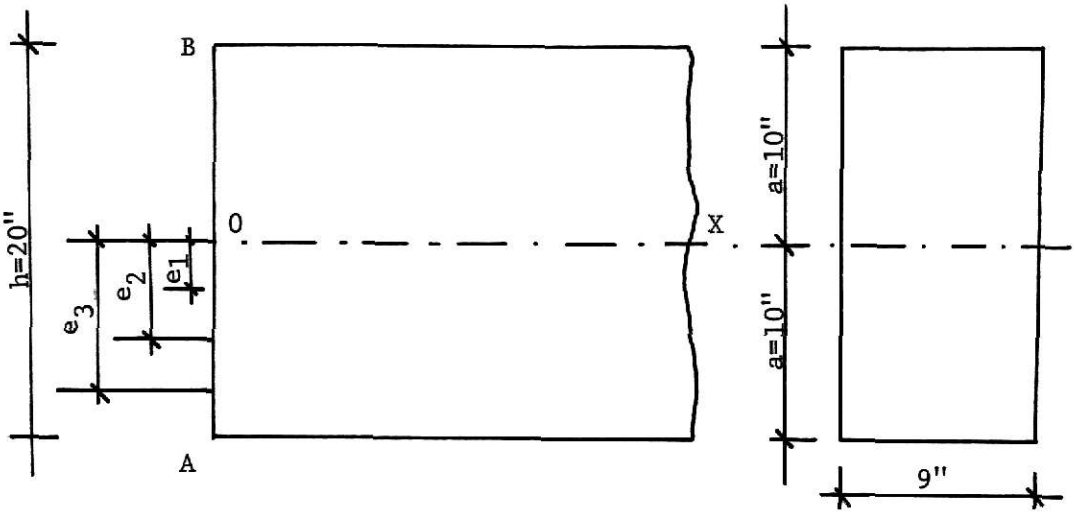

Figure 26. End-block.

Case I. For concentrated load $\frac{a'}{a} = 0$.

A) By Guyon's method.

a) $e = 0$.

Average compression $p = \frac{100 \times 1000}{20 \times 9} = 556$ psi,

using the graph of Fig. 7, for $\frac{a'}{a} = 0$.

Maximum bursting tensile stress $= 0.5p$

$= 0.5 \times 556$

$= 278$ psi

at a distance from loading face is $= 0.32 \frac{h}{2}$

$= 0.32 \times 10 = 3.2"$

Maximum spalling stress [of reference (1)] from Table I $= 0.65\ p = 362$ psi at $\pm \frac{3}{8}$ h from the centroid of beam OX.

b) $e_1 = \frac{h}{8} = 2.5" = \frac{a}{4}$

Using the symmetrical prism method the height of the symmetrical prism

$$h_1 = 2(a - \frac{a}{4}) = \frac{3}{2} a = \frac{3}{4} h = 15"$$

the average compression $p_1 = \frac{100 \times 1000}{15 \times 9} = 740$ psi

Maximum bursting stress $= 0.5p_1$

$= 0.5 \times 740$

$= 370$ psi

at a distance from the loaded face $= 0.32 \frac{h_1}{2} = 0.32 \times 7.5$

$= 2.4"$

Maximum spalling stress = 0.865 p

= 865 x 556

= 482 psi at $\frac{3}{8}$ h from OX.

c) $e_2 = \frac{h}{4} = \frac{a}{2} = 5''$

height of the symmetrical prism

$h_2 = 2(a - \frac{a}{2}) = a = \frac{h}{2} = 10''$ and the

average compression $p_2 = \frac{100 \times 1000}{9 \times 10} = 1110$ psi.

Maximum bursting stress = 0.5 x P_2

= 0.5 x 1110 = 555 psi

at a distance from loaded face = $0.32 \times \frac{h_2}{2}$

= 1.6"

Maximum spalling stress from Table I = 1.258 p

= 1.258 x 556 = 700 psi

at $\frac{3}{8}$ h from OX.

d) $e_3 = \frac{3}{8} h = \frac{3}{4} a$

height of symmetrical prism $h_2 = 2(a - \frac{3}{4} a) = 5''$

$p_3 = \frac{100 \times 1000}{5 \times 9} = 2220$ psi

Maximum bursting stress = 0.5 x 2220 = 1110 psi at a distance

$= 0.32 \frac{h_3}{2} = 0.32 \times \frac{5}{2} = 0.8''$

Maximum spalling stress = 2.176 p = 2.176 x 556 = 1210 psi at $\frac{1}{4}$ h from OX.

B) By using the graph of K. T. Iyengar.

Since the solution of Iyengar's equations required a computer program the writer has made use of Iyengar's graph shown in Fig. 20 and Guyon's symmetrical prism method. As there are no graphs or tables available for computing the spalling stress it remains unknown in this case.

a) $e = 0$

$$p = \frac{100 \times 1000}{20 \times 9} = 556 \text{ psi}$$

$\frac{a'}{a} = 0$ and using graph in Fig. 20c we get a maximum bursting stress $= 0.475\ p = 0.475 \times 556 = 270$ psi at a distance from loaded face $= 0.25\ \frac{h}{2} = 2.5"$.

b) $e_1 = \frac{h}{8} = \frac{a}{4} = 2.5"$

height of symmetrical prism $= 2(a - \frac{a}{4}) = 15"$

$$P_1 = \frac{100 \times 1000}{15 \times 9} = 740 \text{ psi}$$

Maximum bursting stress $= 0.475 \times 740 = 351$ at a distance from the loaded face of $0.25a_1 = 0.25 \times \frac{15}{2} = 1.88"$

c) $e_2 = \frac{h}{4} = \frac{a}{2} = 5"$

height of symmetrical prism $= 2(a - \frac{a}{2}) = 10"$

$$P_2 = \frac{100 \times 1000}{10 \times 9} = 1110 \text{ psi}$$

Maximum bursting stress $= 0.475 \times 1110 = 528$ psi at a distance $= 0.25 \times \frac{10}{2} = 1.25"$

d) $e = \frac{3}{8}\ h = \frac{3}{h}\ a$

height of symmetrical prism = $2(a - \frac{3}{4}a) = 5"$

$$P_3 = \frac{100 \times 1000}{5 \times 9} = 2220 \text{ psi}$$

Maximum bursting stress = 0.475 x 2220 = 1050 psi at a distance from loaded face = $0.25 \times \frac{5}{2} = 0.625"$.

C) By Physical Analog Method.

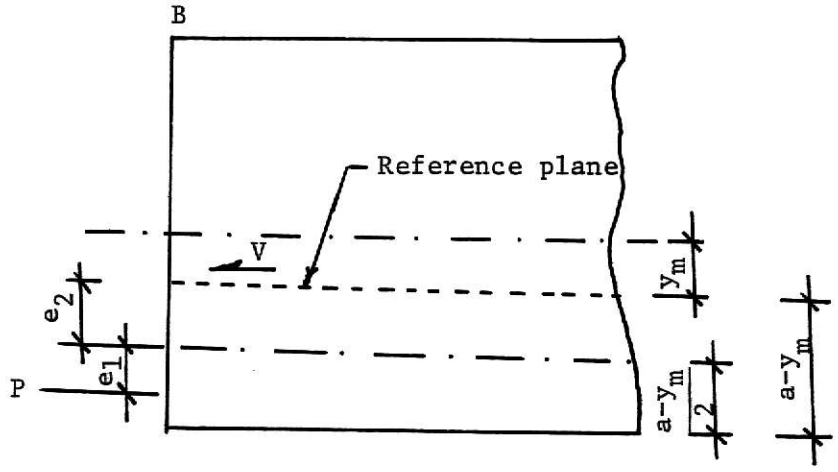

Figure 27. Elevation of end-block.

a) e = 0

To find the maximum bursting stress.

The reference plane coincides with the load axis. The shear acting along the plane is

$$V = P\ (0.5 + \frac{Ym}{h})\ \ 1 - \frac{6e}{h}\ (0.5 - \frac{Ym}{h})$$

$$V = 100000\ (0.5 + \frac{0}{h})\ (1)$$

$$= 100000\ (0.5) = 50{,}000 \text{ lbs.}$$

$$Mp = pe_1 = 100000 \times 0.5 \times 10 = 500000 \text{ lb - in}$$

$$Mv = Ve_2 = -50{,}000 \times 0.5 \times 10 = -250000 \text{ lb - in}$$

$$Mt \frac{I_b}{I} = 0$$

From Eq. (27),

$$Mo = Mp + Mv - Mt \frac{I_b}{I}$$

$$= 500000 - 250000 = 250000 \text{ lb - in}$$

From Eq. (35) $f_{ybc} = Mo \frac{1}{bh_b^2} = 250{,}000 \times \frac{1}{9 \times 10^2} = 278$ psi

To find the maximum spalling stress.

Position of the critical plane by Eq. (36)

$$Ym = \frac{1}{3}(7e - 2h) = -\frac{2}{3}h = 13.33"$$

Here the expression fails to give the position of the critical plane and hence the spalling stress.

b) $e = \frac{h}{8} = 2.5"$

To find the maximum bursting stress.

Reference plane coincides with the load axis.

$$V = p(0.5 + \frac{Ym}{h})\ 1 - \frac{6e}{h}(0.5 - \frac{Ym}{h})$$

$$= 100000\ (0.5 + \frac{1}{8})\ 1 - 0.75\ (0.5 - 0.125)$$

$$= 45000 \text{ lb.}$$

$$Mp = Pe_1 = 100000 \times 0.5 \times (10 - 2.5)$$

$$= 375{,}000 \text{ lb - in}$$

$$Mv = Vxe_2 = -45000 \times 0.5 \times (10 - 2.5)$$

$$= -169000 \text{ lb - in}$$

$$Mt\,\frac{I_b}{I} = -100000 \times 2.5 \times \left(\frac{7.5}{20}\right)^3$$

$$= -13300 \text{ lb - in.}$$

Using Eq. (27),

$$Mo = 375000 - 169000 + 13300 = 219300 \text{ lb - in.}$$

From Eq. (35), $f_{ybc} = Mo\,\frac{1}{bh_b^2} = 219300 \times \frac{1}{9 \times (7.5)^2} = 432$ psi

To find the spalling stress,

$$Ym = \frac{1}{3}(7e - 2h)$$

$$= \frac{1}{3}(17.5 - 40) = -7.5\text{" (i. e. above the centroid of the beam.)}$$

$$V = 100000\left(0.5 + \frac{(-7.5)}{20}\right)\ 1 - 0.75\left(0.5 - \frac{(7.5)}{20}\right)$$

$$= 43000 \text{ lb.}$$

$$Mp = -100000 \times (0.5 \times 17.5 - 7.5)$$

$$= -125000 \text{ lb - in}$$

$$Mv = -43000 \times 0.5 \times 17.5$$

$$= -376000 \text{ lb.}$$

$$Mt\,\frac{I_b}{I} = -100000 \times 2.5\left(\frac{17.5}{20}\right)^3$$

$$= -167000 \text{ lb - in}$$

$$Mo = Mp + Mv - M + \frac{I_b}{I}$$

$$= -125000 - 376000 + 167000 = -334000 \text{ lb - in.}$$

Maximum spalling stress is obtained by using Eq. (34).

$$f_{ys} = -Mo\,\frac{2\ \ 6}{bh_b^2} = 334000 \times \frac{1}{9 \times (17.5)^2}$$

$$= 594 \text{ psi}$$

c) $e = \frac{h}{4} = 5"$

Proceeding similarly as above we find maximum bursting stress

$$f_{ybc} = 626 \text{ psi}$$

Maximum spalling stress

$$f_{ys} = 1150 \text{ psi}$$

d) $e = \frac{3}{8} h$

Maximum bursting stress

$$f_{ybc} = 850 \text{ psi}$$

and maximum spalling stress

$$f_{ys} = 1510 \text{ psi.}$$

Case II.

Using a plate of 3" x 3",

i. e., $2a' = 3"$

A) By Guyon's method.

a) $e = 0$

$$P = \frac{100 \times 1000}{20 \times 9} = 556 \text{ psi}$$

$$\frac{2a'}{2a} = \frac{3}{20} = 0.15$$

By using the graphs of Fig. 7c and 7b we get the maximum bursting stress = 0.4 P = 0.4 x 556 - 222 psi at a distance = 0.58a = 0.58 x 10 = 5.8" from the loaded face.

b) $e = \frac{h}{8} = 2.5"$

Using the symmetrical prism method as in Case I,

$$P_1 = \frac{100 \times 1000}{15 \times 9} = 740 \text{ psi}$$

$$\frac{2a'}{2a} = \frac{3}{15} = 0.2.$$

Maximum bursting stress = 0.36 x 740 = 266 psi at a distance = $0.62a_1$ = 0.62 x 7.5 = 4.65" from the loaded face.

c) $e = \frac{h}{4} = 5"$

$$P_2 = \frac{100 \times 1000}{10 \times 9} = 1110 \text{ psi}$$

$$\frac{2a'}{2a} = \frac{3}{10} = 0.3$$

Maximum bursting stress = 0.31 P_2 = 0.31 x 110 = 344 psi at a distance = 0.72 a_1 = 3.6" from the loaded face.

d) $e = \frac{3}{8} h = 7.5"$

$$P_3 = \frac{100 \times 1000}{5 \times 9} = 2220 \text{ psi}$$

$$\frac{2a'}{2a} = \frac{3}{5} = 0.6"$$

Maximum bursting stress = 0.17 P_3 = 0.17 x 2220 = 376 psi at a distance = 0.88 a_1 = 0.88 x $\frac{5}{2}$ = 2.2" from the loaded face.

B) By using Iyengar's graphs

a) e = 0

Average compression $p = \frac{100 \times 1000}{20 \times 9} = 556$

$$\frac{2a'}{2a_1} = \frac{3}{20} = 0.15$$

Using graphs of Figs. 20c and 20b we get a maximum bursting stress = 0.39 P = 0.39 x 556 = 217 psi at a distance = 0.59 a_1 = 5.9" from the loaded face.

b) $e = \frac{h}{8} = 2.5"$

$$P_1 = \frac{100 \times 1000}{20 \times 9} = 740 \text{ psi}$$

$$\frac{2a'}{2a_1} = 0.2$$

Maximum bursting stress = $0.355\ P_1 = 263$ psi at a distance = $0.65\ a_1 = 4.87"$ from the loaded face.

c) $e = \frac{h}{4} = 5"$

$$P_2 = \frac{100 \times 1000}{10 \times 9} = 1110 \text{ psi}$$

$$\frac{2a'}{2a_1} = \frac{3}{10} = 0.3$$

Maximum bursting stress = $0.3\ P_2 = 0.3 \times 1110 = 333$ psi at a distance = $0.73\ a_1 = 3.65"$ from the loaded face.

d) $e = \frac{3}{8}\ h = 7.5"$

$$P_3 = \frac{100 \times 1000}{5 \times 9} = 2220 \text{ psi}$$

$$\frac{2a'}{2a_1} = \frac{3}{5} = 0.6$$

Maximum bursting stress = $0.165\ P_3 = 366$ psi at a distance $0.88\ a_1 = 2.2"$ from the loaded face.

C) By physical analog method.

a) $e = 0$

In case I we have found

$f_{ybc} = 278$ psi

using Eq. (37a) $t = 2a' = 3"$ size of plate.

$$f_{yb} = f_{ybc}\ 1 - \frac{t}{h}\ (3 - 4\ \frac{h_b}{h})$$

$$= 278\ \ 1 - \frac{3}{20}\ (3 - 4\ \frac{10}{20})$$

$$= 236 \text{ psi}$$

b) $e = \frac{h}{8}$

$$f_{ybc} = 432 \text{ psi}$$

$$f_{yb} = 432\ \ 1 - \frac{3}{20}\ (3 - 4\ \frac{7.5}{20})$$

$$= 327 \text{ psi}$$

c) $e = \frac{h}{4}$

$$f_{ybc} = 626 \text{ psi}$$

$$f_{yb} = 626\ \ 1 - \frac{3}{20}\ (3 - 4\ \frac{5}{20}) \ = 438 \text{ psi}$$

d) $e = \frac{3}{8}\ h$

$$f_{ybc} = 850 \text{ psi}$$

$$f_{yb} = 850\ \ 1 - \frac{3}{20}\ (3 - 4\ \frac{2.5}{20}) \ = 531 \text{ psi}$$

Results of Example 1.

TABLE II. Maximum bursting stress along the axis of the concentrated load as found by three methods.

No.	e	Guyon		K. T. Iyengar		Physical analog	
		Stress in lb/sq in.	Position of f_{ybc} from AB	Stress in lb/sq in.	Position of f_{ybc} from AB	Stress in lb/sq in.	Position of f_{ybc} from AB
1	0	278	3.2"	270	2.5"	298	--
2	$\frac{h}{8}$	370	2.4"	351	1.88"	432	--
3	$\frac{h}{4}$	555	1.6"	528	1.25"	626	--
4	$\frac{3}{8}$ h	1110	0.8"	1050	0.625"	850	--

TABLE III. Maximum bursting stress along the axis of the distributed load found by three methods.

No.	e	Guyon		K. T. Iyengar		Physical analog	
		Stress in lb/sq in.	Position of f_{ybc} from AB	Stress in lb/sq in.	Position of f_{ybc} from AB	Stress in lb/sq in.	Position of f_{ybc} from AB
1	0	222	5.8"	217	5.9"	236	--
2	$\frac{h}{8}$	266	4.65"	263	4.87"	327	--
3	$\frac{h}{4}$	344	3.6"	333	3.65"	438	--
4	$\frac{3}{8}$ h	376	2.2"	366	2.2"	531	--

TABLE IV. Maximum spalling stress.

No.	e	Guyon	Physical analog
1	0	362 psi	--
2	$\frac{h}{8}$	482 psi	594 psi
3	$\frac{h}{4}$	700 psi	1150 psi
4	$\frac{3}{8}$ h	1210 psi	1510 psi

Example 2

The amount of reinforcement required in Example 1 for e = 0 and with a bearing plate is computed as shown below. Assume the tensile strength of concrete, f_t = 240 psi and the tensile strength of stirrups to be 20,000 psi.

1) By Guyon's method.

From Example 1 the maximum bursting stress = 278 psi at 3.2" from AB (loaded face). The positions of zero stresses are at zero and at 20". The approximate distribution of f_y may be drawn as shown in Fig. 28. The apex of the triangle is at a point 10% higher than the maximum bursting stress = 278 x 1.1 = 306 psi to form approximate triangle. The tensile force per unit width = 1/2 x 20 x 306 = 3060 lb. Therefore for 9" width = 3060 x 9 = 27,600 lb.

Since we are allowing 240 psi tension in concrete, the reinforcement should be provided for the tensile force under the hatched area of Fig. 28 alone.

The hatched area is given by

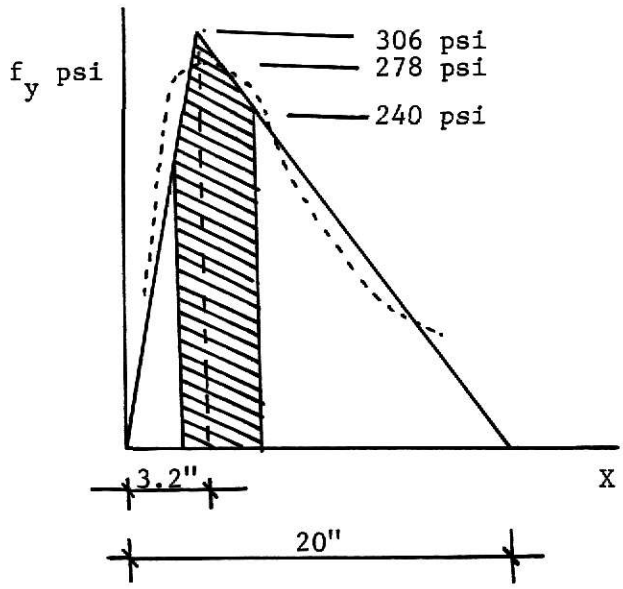

Figure 28. Approximate triangular distribution of f_y.

$$S\left[1 - \left[\frac{f_t}{f_y}\ \text{max}\right]^2\right]$$

therefore the force to be carried by reinforcement

$$= 27600\left[1 - \left(\frac{240}{306}\right)^2\right]$$

$$= 10700 \text{ lb.}$$

and the area of the steel needed = $\frac{10700}{20000}$ = 0.535 sq. inch using No. 3 bars (A = 0.11 sq. inch).

No. of bars required = $\frac{0.535}{0.11}$ = 5 bars.

Therefore one must provide No. 3 bars at $1\frac{3}{4}$" centers placed vertically parallel to the bearing surface at the point of maximum stress. Also No. 3 bars at 4" centers are placed in a horizontal position as shown in Fig. 29.

Guyon assumes the maximum spalling force to be .04P = .04 x 100000 = 4000 lb. so the area of steel = $\frac{4000}{20000}$ = 0.2 sq. inch. Therefore one must

provide 2 No. 3 bars at the top and bottom of the block as shown in Fig. 29.

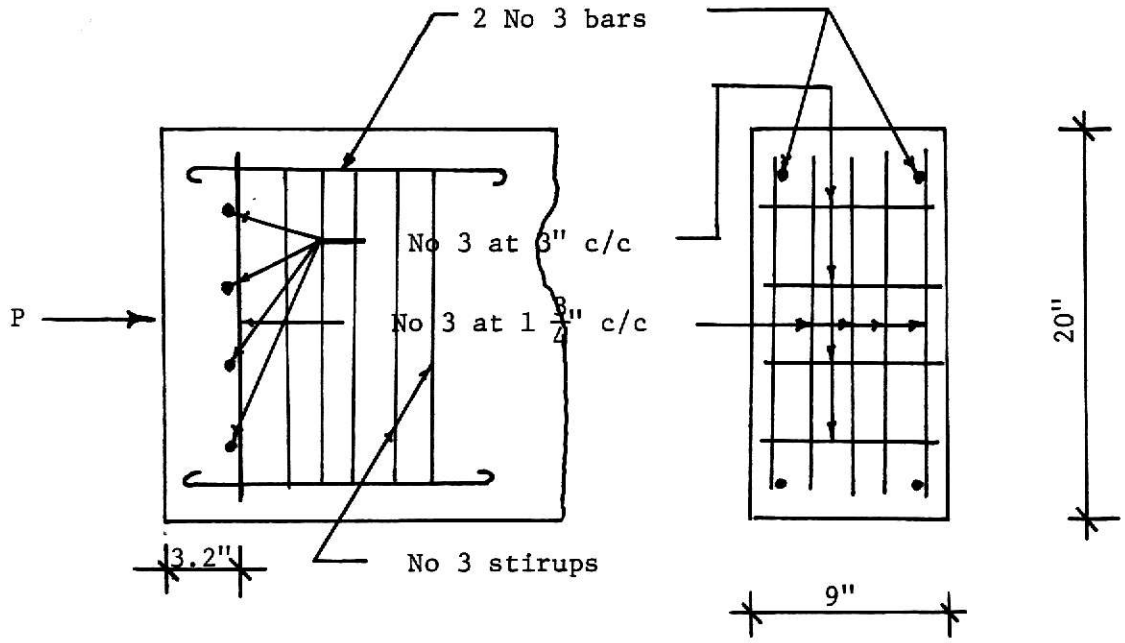

Figure 29. Position of reinforcement in end-block for example 2.

2) By the physical analog method.

Eq. (40) gives the force in the reinforcement to prevent bursting crack as

$$fo = \frac{Mo}{h_b^2}\left(1 - \frac{f_t}{f_{yb}}\right)$$

$$fo = \frac{250000}{100}\left(1 - \frac{240}{278}\right)$$

$$= 350 \text{ lb. per inch.}$$

Here the authors R. J. Lenschow and M. A. Sozen do not specify the exact position and length of the end-block for which reinforcement should be provided.

CONCLUSIONS

After studying these methods and solving numerical examples by these three methods we are in a position to make the following conclusions.

1) The work of Guyon very nearly tallies with the more exact analysis given by K. T. Iyengar; also from the graph in Fig. 33, it can be seen that it errs on the side of safety.

2) Guyon has given importance to the transverse stress only and he used it to calculate the reinforcement in end blocks, while the stress which actually causes failure is that due to the principal tensile stress which can be calculated from known transverse, longitudinal and shear stress, but it is found that the principal tensile stress is very nearly and, in some cases, exactly equal to the transverse stress. Hence Guyon's consideration of transverse stress is justified. Again it saves laborious calculation of longitudinal and shear stress which are very important in practical applications.

3) From the work of K. T. Iyengar and the graph in Fig. 20 given by him we can see that the transverse stresses become almost zero at a distance equal to the depth of the beam. Hence the assumption made by Guyon and some of the other workers that stress becomes purely longitudinal at a distance equal to the depth of the beam is justified.

4) Consider the results of the examples solved in this report. From Table II we see that, for the first three cases, the physical analog gives a higher stress than Guyon's method, but suddenly and at a higher eccentricity, e. g., at $e = \frac{3}{8} h$ it gives a stress about 23% lower than Guyon's method. Hence this

shows that the equation given by physical analog should be verified before it is used for practical analysis. On comparing the result of Example 1 for $e = \frac{3}{8} h$ with that of the graph in Fig. 30 it can be verified that the physical analog method gives lower stresses than Guyon's method. The same graph shows that Iyengar's stresses are higher than Guyon's which does not tally with the result of Example 1, probably due to unavailability of the proper table; the symmetrical prism method may not be applicable in his case.

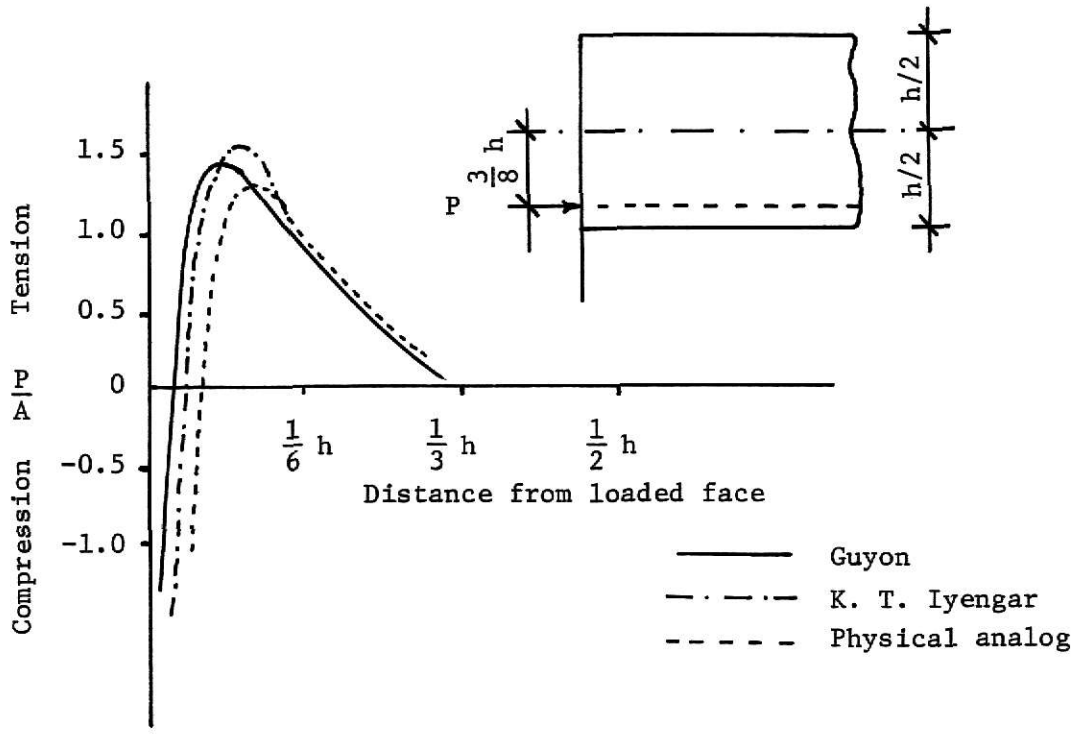

Figure 30. Comparison of transverse stress distribution along axis of load.

5) Equation (40) gives maximum bursting stress but does not give its exact position as in the case of Guyon or K. T. Iyengar; also we do not know the correct distribution of stress. If we assume the maximum stress throughout the block it will result in a very conservative design.

6) On comparing the position of the plane of maximum spalling stress

given by Guyon and physical analog, with different eccentricities as given in Table V below, we find that they do not agree; also in the case of e = 0 the physical analog method does not give the spalling stress.

TABLE V. Position of the plane of maximum spalling stress from mid-height of end-block.

	1	2	3
No.	e	Guyon	Physical analog
1	0	$\pm \frac{3}{8}$ h	--
2	$\frac{h}{8}$	$\frac{3}{8}$ h	$-\frac{3}{8}$ h
3	$\frac{h}{4}$	$\frac{3}{8}$ h	$-\frac{1}{12}$ h
4	$\frac{3}{8}$ h	$\frac{1}{4}$ h	$\frac{5}{24}$ h

Column 2 obtained from Reference 1, Appendix I, Table I.

Column 3 obtained from Eq. (36).

7) It can be seen from the solved problem that both the bursting and the spalling stresses increase as the eccentricity increases.

8) For small eccentricities the maximum tensile stress is in the bursting zone while for large eccentricities it shifts into the spalling zone. The spalling stresses always act on a smaller area and hence the corresponding forces remain small.

9) From graphs in Figs. 7 and 20 it can be seen that according to Guyon as well as K. T. Iyengar that the transverse stresses are decreasing as the size of the loading plate increases.

10) From Table II it can be seen that the position of the maximum

bursting stress comes nearer to the loaded end with increasing eccentricity and with distributed load. This can also be noticed by examining the isobars of Fig. 8.

(11) The tensile stresses are close to the end face in the spalling zone while they are at a distance from the edge in the bursting zone. This can be verified from the general transverse stress diagram Fig. 31a,b as shown below.

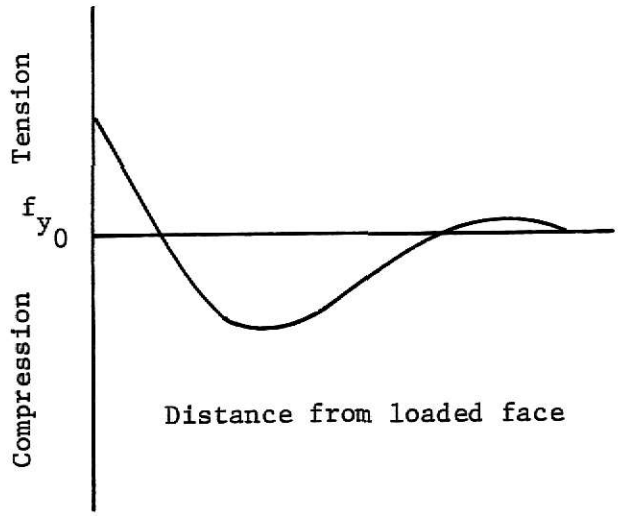

Figure 31a. Distribution of transverse stress for bursting zone.

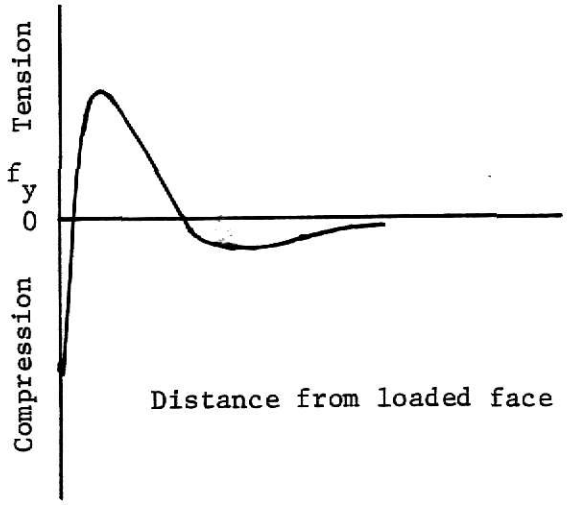

Figure 31b. Distribution of transverse stress for spalling zone.

12) It can be seen that Guyon as well as Iyengar made a two-dimensional analysis and that the third dimension was not considered. Also, the effects of the cable ducts are not accounted for; but on studying the two- and three-dimensional photoelastic experiment carried out by S. P. Christodoulides[6][7] and plotting the graphs in Figs. 32[2] and 33[2] we observe that the transverse stresses given by Guyon and Iyengar are very low. According to K. T.

Iyengar the higher value of photoelasticity can be due to approximation in the numerical work done after photoelastic experiments, which gives only a difference of principal stresses.

13) As far as reinforcement in the block is concerned, it should be provided in two directions normal to the axis of the load. In case of inclined forces it is not practicable to provide reinforcement normal to the axis of the load, but in such a case it is normal to the axis of the beam. Helical reinforcement can be a better solution.

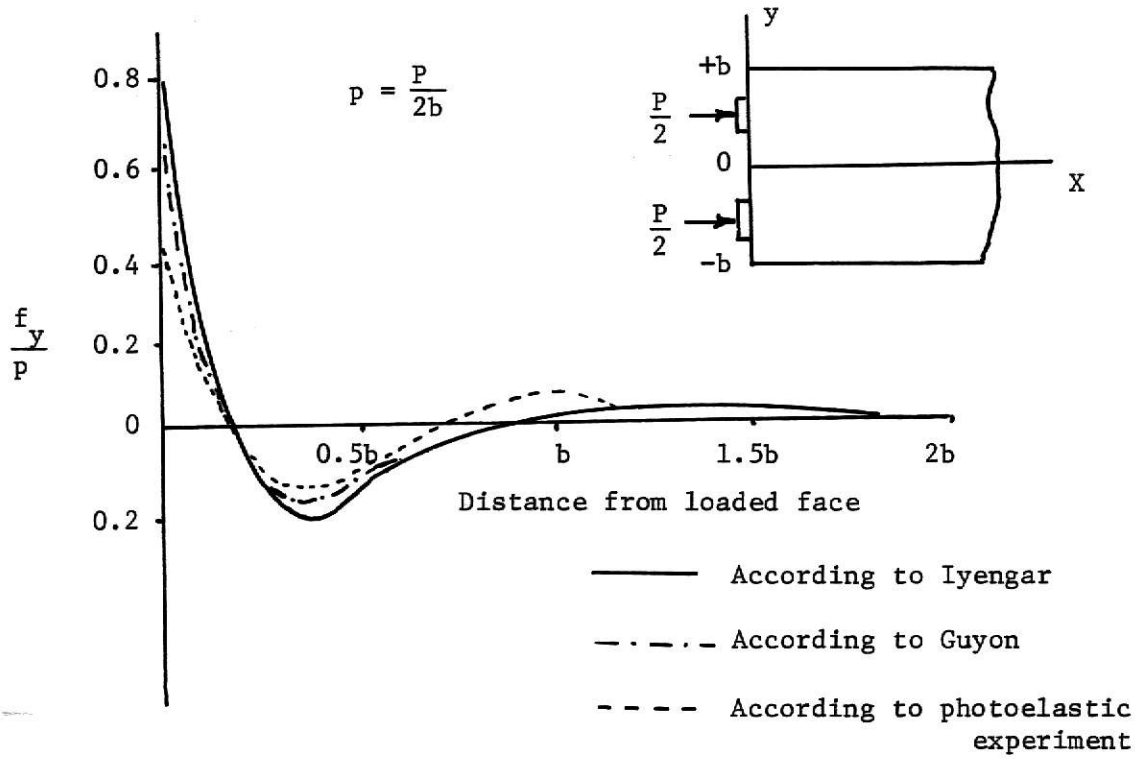

Figure 32. Distribution of transverse stress along y = o for two symmetrical forces.

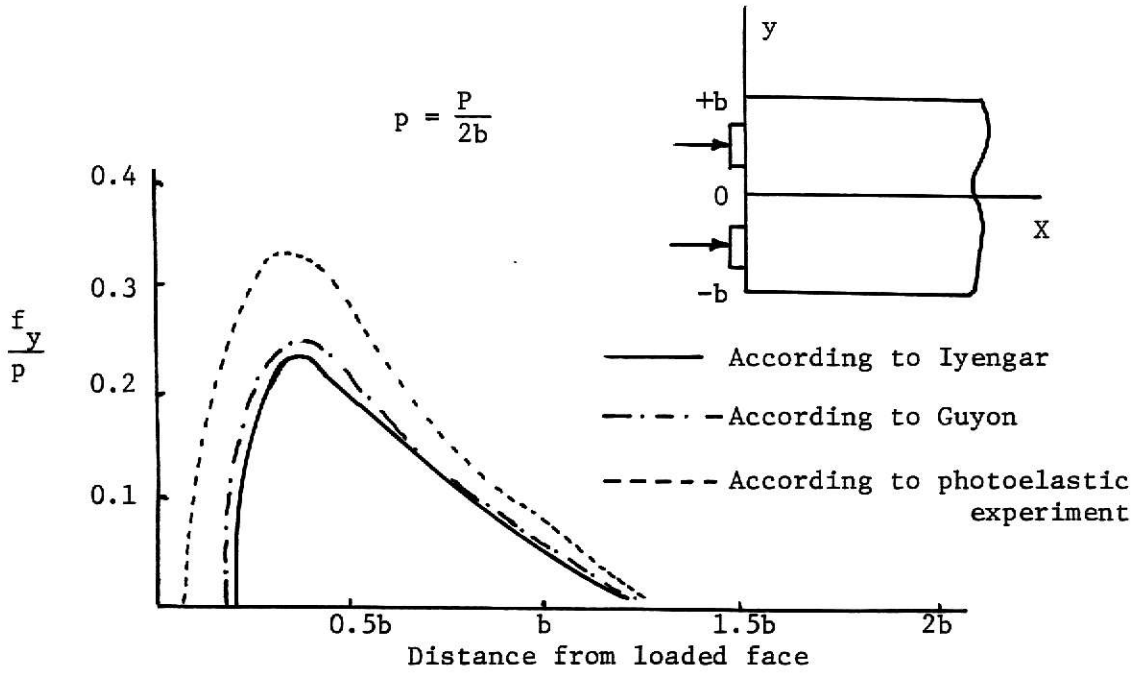

Figure 33. Distribution of transverse stress f_y along y = ±b/2 for two symmetrical forces.

BIBLIOGRAPHY

(1) Guyon, Y., Prestressed concrete. Vol. I. John Wiley and Sons, Inc., New York, 1960.

(2) Sundra Raja Iyengar, K. T., "Two-dimensional theories of Anchorage Zone Stresses in Post-tensioned Prestressed Beams." ACI Journal, Proceedings, v. 59, No. 10, Oct. 1962. pp. 1443-1466.

(3) Sundra Raja Iyengar, K. T., "On a Two-Dimensional Problem in the End-Block Design of Post-tensioned Prestressed Concrete Beams." Proceedings, 1st Congress of Teoratical and Applied Mechanics, Kharagpur (India) 1955. pp. 107-112.

(4) R. J. Lenschow and M. A. Sozen. "Practical Analysis of the Anchorage Zone Problem in Prestressed Beams." ACI Journal, Proceedings, v. 62, No. 11, Nov. 1965. pp. 1421-1439.

(5) K. Chandrashekhara and N. Raghavendra, "Practical Analysis of the Anchorage Zone Problem in Prestressed Beams." ACI Journal, Proceedings, v. 63, No. 6, June 1966. pp. 1813-1817.

(6) Christodoulides, S. P., "A Two-dimensional Investigation of the End Anchorages of Post-tensioned Concrete Beams." The Structural Engineer (London), v. 33, No. 4, 1955. pp. 120-133.

(7) Christodoulides, S. P., "The Distribution of Stresses around the End Anchorages of Prestressed Concrete Beams. Comparison of Results Obtained Photoelastically with Strain Gauge Measurements and Theoretical Solutions." Publication, International Association for Bridge and Structural Engineering, v. 16, 1956. pp. 55-70.

(8) J. P. Den Hartog, "Advanced Strength of Materials." McGraw-Hill Book Company, Inc., New York, 1952.

(9) Pickett, G. and Sundra Raja Iyengar, K. T., Stress Concentration in Post-tensioned Prestressed Concrete Beams. Journal of Technology (Calcutta), v. 1, No. 2, 1956. pp. 105-112.

ACKNOWLEDGMENT

I would like to express my wholehearted gratitude to Professor Vernon H. Rosebraugh, Associate Professor of Civil Engineering at Kansas State University, for his valuable advices and encouragement, and to Dr. Jack B. Blackburn, Head of Civil Engineering department, Dr. Peter B. Cooper, Dr. Stuart E. Swartz and Leonard E. Fuller for serving on my committee.

A STUDY OF END-BLOCKS FOR POST-TENSIONED BEAMS

by

TAHER F. GINWALA

B. E. (Civil), Poona University, India, 1969

AN ABSTRACT OF A MASTER'S REPORT

submitted in partial fulfillment of the

requirements for the degree

MASTER OF SCIENCE

Department of Civil Engineering

KANSAS STATE UNIVERSITY
Manhattan, Kansas

1970

The stress distribution in end-blocks of post-tensioned prestressed concrete beams has become important due to extensive use of prestressed concrete beams. An attempt has been made to present the research work of some predominant authorities on this topic in this writing.

The following three approaches have been identified in this report: 1) the two-dimensional analysis by Y. Guyon, 2) the two-dimensional analysis by Sundra Raja Iyengar, and 3) the physical analog method by R. J. Lenschow and M. A. Sozen.

Finally, comparison of these methods has been made by solving numerical examples. The methods are also compared with a photoelastic investigation by S. P. Christodoulides.